THE DYNAMO EFFECT

S. FAUVE AND F. PETRELIS

LPS, Ecole normale supérieure,
24, rue Lhomond,
75005 Paris, France
E-mail: fauve@lps.ens.fr

We first present basic results about advection, diffusion and amplification of a magnetic field by the flow of an electrically conducting fluid. This topic has been initially motivated by the study of possible mechanisms to explain the magnetic fields of astrophysical objects. However, self-generation of a magnetic field by an electrically conducting fluid, the so-called dynamo effect, is also a typical bifurcation problem that involves many interesting aspects from the viewpoint of dynamical system theory: the effect of the flow geometry on the nature of the bifurcation, the effect of turbulent fluctuations on the threshold value, the saturation mechanisms above threshold, the dynamics of the generated magnetic field and the statistical properties of its fluctuations with respect to the ones of the turbulent flow. We have tried to emphasize some of these problems within the general presentation of the subject and more particularly in sections 6 and 7. These notes should not be considered as a review article. There exist many well known books and reviews on dynamo theory [1,2,3,4,5,6]. For a general presentation of the subject, we refer to "Magnetic field generation in electrically conducting fluids" by Moffatt [7]. The generation of large scale magnetic fields by small scale turbulent motions is reviewed in "Mean-field magnetohydrodynamics and dynamo theory" by Krause and Rädler [8]. The problem of "fast dynamos" in the limit of large magnetic Reynolds number is studied by Childress and Gilbert in "Stretch, twist, fold: the fast dynamo" [9]. Finally, we refer to "Magnetic fields in astrophysics" by Zeldovich, Ruzmaikin and Sokoloff [10] for a detailed review on magnetic fields of astrophysical objects and their possible role in the early evolution of the universe.

1. Introduction: from industrial dynamos to the magnetic field of stars and planets

1.1. *Generation of an electric current by a rotating conductor*

The generation of an electric current from mechanical work is a very common process. Most of the electric energy we are using on the Earth has been transformed from mechanical energy at some stage. It is however not always understood that the elementary process that allows the trans-

formation of mechanical work into electromagnetic energy is an instability mechanism.

It has been known since Faraday that it is possible to generate an electric current by rotating an electrically conducting disk of radius a in an externally applied magnetic field $\vec{B}_0$ (see Figure 1 a). Indeed, the electromotive force e between the points A and P can be easily computed from the law of induction

$$e = \int_{AP} \left((\vec{\Omega} \times \vec{r}) \times \vec{B}_0 \right) \cdot d\vec{r} = \frac{1}{2} \Omega a^2 B_0, \tag{1}$$

and generates a current $I = e/R$ in the electric circuit of resistance R. Is it possible to use this current to generate the magnetic field $\vec{B}_0$? This may look a strange question but leads to a typical instability problem. The answer is yes if the geometry of the circuit is such that a perturbation of the electrical current generates a magnetic field which amplifies the current by electromagnetic induction. An experimental demonstration of this type of effect was first performed by Siemens [11] and gave rise to various devices widely used to generate an electrical current from mechanical work. The simplest although non efficient way to achieve self-generation of a current or a magnetic field is the homopolar dynamo displayed in Figure (1 b) (sometimes called the Bullard dynamo in the english literature). Ohm's law gives

$$L\frac{dI}{dt} + RI = e = M\Omega I, \tag{2}$$

where L is the induction of the circuit and M is the mutual induction between the wire and the disk. Indeed, from equation (1) it follows that e is proportional to Ω and I that generates the magnetic field $\vec{B}$. Using equation (2), the stability analysis of the solution $I = 0$ (corresponding to $B = 0$) is straightforward. The current I and thus the magnetic field B are exponentially amplified if

$$\Omega > \Omega_c = \frac{R}{M}. \tag{3}$$

It first appears that the self-generation of current depends on the sign of the rotation rate. This is not very surprising because the wire breaks the mirror symmetry with respect to any plane containing the axis of rotation. The sign of the wire helicity gives the sign of M and thus determines the sign of Ω for self generation. Note that if we add a second wire of opposite helicity parallel to the first one such that the device becomes mirror symmetric, then $M = 0$ and self-generation of current is no longer possible. We
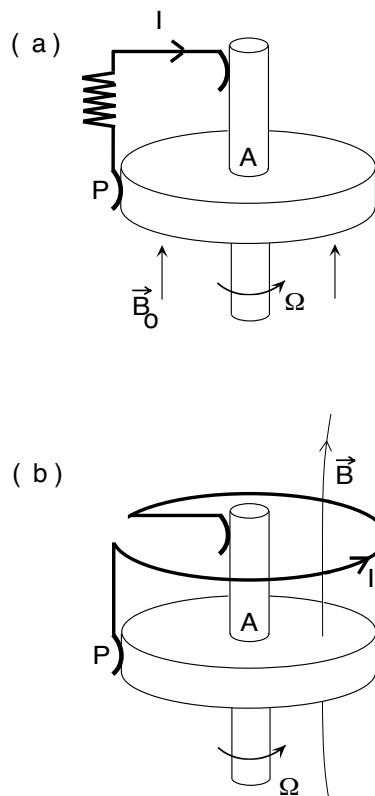
Figure 1.   (a) Sketch of the Faraday inductor. (b) Sketch of the homopolar dynamo.

will also observe that broken mirror symmetry by the flow is important in the case of fluid dynamos. We have obtained so far the condition (3) for the onset of dynamo action. This is called solving the kinematic dynamo problem. For a rotation rate larger than Ω_c, equation (2) seems to indicate that the current is exponentially growing. This process should stop at some stage as shown by the equation for the angular rotation rate

$$J\frac{d\Omega}{dt} = \Gamma - D - MI^2,\qquad(4)$$

where J is the moment of inertia of the disk, Γ is the torque of the motor driving the disk, D represents mechanical resistive torques. The last term is the torque which results from the Laplace force generated by the magnetic

field $\vec{B}$ acting on the current density $\vec{j}$ flowing in the disk

$$\int \vec{r} \times \left(\vec{j} \times \vec{B} \right) d^3r = MI^2 \, \hat{z}. \tag{5}$$

This force is opposite to the motion of the disk and is proportional to I^2. It can be easily checked that the proportionality constant in (5) is M by looking at the energy budget. To wit, we multiply (2) by I and (4) by Ω and add them. We obtain

$$\frac{d}{dt} \frac{1}{2} \left(J\Omega^2 + LI^2 \right) = (\Gamma - D)\,\Omega - RI^2. \tag{6}$$

This equation reflects energy conservation. In a stationary regime, the power of the motor is dissipated by mechanical losses and Joule heating. Note that the two contributions proportional to ΩI^2 cancel in order to have energy conservation. The growth of the current is thus limitated by the available mechanical power. The stationary solutions of equations (2, 4) are

$$\Omega = \Omega_c = \frac{R}{M}, \quad I = \frac{\Gamma - D}{R}\Omega = \frac{\Gamma - D}{M}. \tag{7}$$

Finding the generated current or magnetic field is called solving the dynamic dynamo problem. The kinematic dynamo problem is thus the linear stability analysis of the solution $B = 0$ whereas the dynamic dynamo problem consists of solving the full nonlinear problem.

In the above simple example, we have a stationary bifurcation for $\Omega = \Omega_c$. The broken symmetry at instability onset is the $B \to -B$ symmetry or the $I \to -I$ symmetry of equations (2, 4). The bifurcation diagram may look surprising. The bifurcated branches of solution for I that we expect for $\Omega > \Omega_c$ are absent. This is because we have neglected all the possible nonlinear saturation mechanisms (dependence of L or M on B, destruction of the circuit if I becomes too large, detailed behavior of the motor, etc). However, this example shows how the dynamo effect allows to generate electromagnetic energy from mechanical work. A lot of its features will subsist in fluid dynamos i.e. generation of a magnetic field by the motion of an electrically conducting liquid.

1.2. *Magnetic fields of astrophysical objects*

Magnetic fields exist on a wide range of scales in astrophysics. We will just recall here some results and refer to a review of this topic [10]. Orders of magnitude of the magnetic fields and some associated relevant parameters for planets, stars and our galaxy are given in Table 1.

Table 1. Magnetic fields and fluid parameters of astrophysical objects. All quantities are given in MKSA units except the magnetic diffusion time L^2/ν_m which is given in years.

Medium	B	ρ	L	ν_m	$\frac{L^2}{\nu_m}$	$\frac{B^2 L^3}{2\mu_0}$	$\frac{B^2 L \nu_m}{2\mu_0}$
Our galaxy	10^{-10}	$2\,10^{-21}$	10^{19}	10^{17}	10^{13}	10^{43}	10^{22}
Sun	10^{-4}	1	$2\,10^8$	10^3	10^6	$4\,10^{22}$	10^9
Jupiter	$4\,10^{-4}$	10^3	$5\,10^7$	10	10^7	10^{22}	$4\,10^7$
Earth	10^{-4}	10^4	$3\,10^6$	3	10^5	$2\,10^{17}$	10^5
White dwarfs	$10^2 - 10^4$	10^{10}	10^7				
Neutron stars	10^6 - 10^9	10^{19}	10^4				

It is perhaps meaningless to try to compare these data because these astrophysical objects have strongly different physical properties. A magnetohydrodynamic description is probably valid for the Earth core which is made of liquid metal, but classical hydrodynamics certainly breaks down both for rarefied plasmas where the mean free path is no longer small compared to the characteristic length on which the velocity varies, and for very dense stars where quantum and relativistic effects are important (see section 2 for a discussion of MHD approximation). If we try anyway to tell something about these data, we may observe that the magnetic field B is not strongly related to the size of the object L but seems to increase with its density ρ. If instead of looking at the intensity of the magnetic field, we consider the typical magnetic energy of the object $B^2L^3/2\mu_0$ (μ_0 is the magnetic permeability of vacuum), we find the expected ordering from the galaxy to the Earth. We may also consider the typical value of the Joule dissipation. To wit, we divide the magnetic energy by the characteristic magnetic diffusion time L^2/ν_m, with $\nu_m = (\mu_0\sigma)^{-1}$ where σ is the electrical conductivity of the medium. We thus get an idea of the amount of power which is necessary to maintain the magnetic field against Joule dissipation. Again, we observe the expected ordering from the galaxy to the Earth. Note that these powers have been certainly underestimated. First, they are estimated from the visible part of the magnetic field. If we consider a celestial body with a nearly axisymmetric mean magnetic field, as it is often the case, Ampère's law shows that the azimuthal component of the magnetic field should vanish out of the conducting medium. If the azimuthal field inside the body is large compared to the poloidal one, we may strongly underestimate the total energy or Joule dissipation by taking the value of the observed poloidal field to evaluate B. Second, we have assumed that the length scale of the gradients of the magnetic field is the

size L of the conducting medium. Magnetic energy at smaller scales will lead to a shorter diffusion time scale and thus to a higher dissipated power. However, even if we multiply the dissipated power by a factor 1000, we still get orders of magnitude rather small compared to the typical energy budgets of the corresponding astrophysical objects.

The very large astrophysical scales lead to long diffusion times L^2/ν_m for the magnetic field. On shorter time scales, we may ignore magnetic diffusivity. The magnetic field is then advected by the flow. If we consider a field tube of section dS and length dl, the corresponding fluid mass, $\rho dSdl$, and the flux of the magnetic field, BdS, are conserved. This leads to $B/\rho \propto dl$. For an isotropic compression, we get $B \propto \rho^{2/3}$. The "relict field hypothesis" is based on this argument. It is argued that a very small intergalactic magnetic field may thus explain the value of the field of our galaxy. A more detailed analysis seems to rule out this possibility [10]. The situation is clearer for the magnetic fields of the sun or planets. Even without invoking turbulent diffusivity, the age of the magnetic field of these objects is in general much larger than their Joule dissipation time scale. Moreover, these magnetic fields have often a complex dynamics in time and space: a roughly 22 year oscillation for the sun and random field reversals for the Earth. Consequently, one should find a field generation mechanism which involves such dynamics.

1.3. *Fluid dynamos*

In a short communication made in september 1919, Larmor observed that the magnetic fields of "celestial bodies" may be generated by internal motions of conducting matter [12]. He emphasized the case of the sun but also considered the magnetic field of the Earth and ruled out other mechanisms that were put forward at that time: rotation of an electric polarization induced either by gravity or centrifugal forces, or of crystalline nature in the case of the Earth. He explained the fluid dynamo mechanism in a few lines; assuming the existence of an initial perturbation of magnetic field, he observed that "internal motion induces an electric field acting on the moving matter: and if any conducting path around the solar axis happens to be open, an electric current will flow round it, which may in turn increase the inducing magnetic field. In this way it is possible for the internal cyclic motion to act after the manner of the cycle of a self-exciting dynamo, and maintain a permanent magnetic field from insignificant beginnings, at the expense of some of the energy of the internal circulation. Again, if a sunspot is regarded as a superficial source or sink of radial flow of strongly ionized material, with the familiar vortical features, its strong magnetic

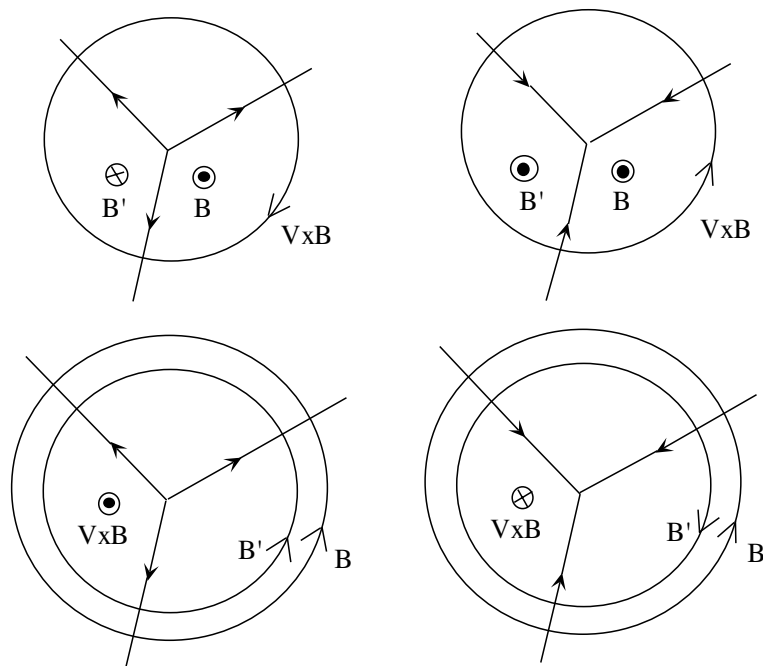field would, on these lines, be a natural accompaniment ..." We can illus-

Figure 2.   Induced magnetic field B' generated by an axial field B applied to a diverg-
ing, (a), respectively converging flow, (b). Induced magnetic field B' generated by an
azimuthal field B applied to a diverging, (c), respectively converging flow, (d).

trate this last sentence by looking at the radial velocity fields $\vec{V}$ of Figure 2.
There is of course an inflow or an outflow at the origin, perpendicular to the
plane of the figure, that we do not take into account. In each case, we have
considered a perturbation of the magnetic field, $\vec{B}$, and we have plotted the
induced magnetic field $\vec{B}'$ generated by the induced current proportional to
$\vec{V} \times \vec{B}$. It seems that an axial field is inhibited by a diverging flow ($B > 0$
and $B' < 0$ in Figure 2a) and amplified by a converging flow ($B > 0$ and
$B' > 0$ in Figure 2b). On the contrary, an azimuthal field appears to be
amplified by a diverging flow (Figure 2 c) and inhibited by a converging
flow (Figure 2 d). Thus, the amplification process strongly depends on the
sign of the velocity field, and as in the case of the homopolar dynamo, the
process is not invariant under the $\vec{V} \rightarrow -\vec{V}$ transformation. Our analysis
of the induction processes of the flows of Figure 2 is very rough: we have
not tried to determine if there is an electric field in addition to the induced

$\vec{V} \times \vec{B}$ field; as said above, we have not taken into account the inflow or outflow at the origin that would make the flow three-dimensional. However, we have illustrated with these simple flows what Larmor had already probably in mind, i.e. that a given flow may amplify some field configurations and at the same time inhibit some others. The main difficulty is that the field geometry is not determined by the geometry of the currents like in the homopolar dynamo or industrial dynamos. As said above, it is for instance enough to modify the homopolar dynamo by adding a second wire, mirror symmetric to the first one to suppress self-generation at any rotation rate. In fluid dynamos, the electrical conductivity is usually constant in the whole flow volume; the dynamo is said "homogeneous" and the current geometry is not prescribed. This makes the dynamo problem much more difficult to solve. In addition, contrary to the case of the homopolar dynamo, it is not obvious that the local amplification of a magnetic field perturbation leads to self-generation. In the examples of Figure 2, the geometry of the amplified magnetic mode can be easily determined by considering the effect of the advection of a magnetic field tube; one has amplification when the advection by the flow makes the magnetic tube thinner. This is just a consequence of the conservation of magnetic flux and may not correspond to the increase of the total magnetic energy at the expense of mechanical work. There are indeed many flow configurations which strongly amplify an externally applied magnetic field in some regions without leading to self-generation.

2. The MHD approximation

2.1. *The approximations and equations of magnetohydrodynamics*

We consider an electrically conducting fluid such as a liquid metal or a plasma. The medium at rest is electrically neutral and there are no externally applied fields or currents. The aim of this paragraph is to derive the MHD equations that approximately govern the magnetic field in a flow of liquid metal.

The electric $\vec{E}$ and magnetic $\vec{B}$ fields are governed by Maxwell's equations

$$\vec{\nabla} \cdot \vec{E} = \frac{\rho_e}{\epsilon_0}, \tag{8}$$

$$\vec{\nabla} \times \vec{E} = -\frac{\partial \vec{B}}{\partial t}, \tag{9}$$

$$\vec{\nabla} \cdot \vec{B} = 0, \tag{10}$$

$$\vec{\nabla} \times \vec{B} = \mu_0 \vec{j} + \frac{1}{c^2} \frac{\partial \vec{E}}{\partial t}, \tag{11}$$

where ρ_e and $\vec{j}$ are the charge and current densities, ϵ_0 and μ_0 are the electric and magnetic permitivities of vacuum and c is the velocity of light. We expect that the spatial and the temporal scales of the electromagnetic fields will be of the same order of magnitude as the ones of the flow. We thus have from (9), $E \sim VB$ where V is the characteristic fluid velocity, and consequently the displacement current in (11) is of order $(V/c)^2$ compared to the other terms. Therefore we have

$$\vec{\nabla} \times \vec{B} \approx \mu_0 \vec{j}. \tag{12}$$

To the same degree of approximation, we use classical laws of transformation of fields to find the electric field $\vec{E}'$ and the magnetic field $\vec{B}'$ in the reference frame of a fluid particle moving at velocity $\vec{v}$,

$$\vec{E}' \approx \vec{E} + \vec{v} \times \vec{B}, \tag{13}$$

$$\vec{B}' \approx \vec{B}. \tag{14}$$

Since the current density $\vec{j}$ does not depend on the reference frame in the classical limit, we get Ohm's law

$$\vec{j} \approx \sigma \left(\vec{E} + \vec{v} \times \vec{B} \right), \tag{15}$$

where σ is the electrical conductivity of the fluid. We assume that σ is constant (see below). Taking the curl of equation (15) and using (10), (9) and (12), we get the evolution equation of the magnetic field

$$\frac{\partial \vec{B}}{\partial t} \approx \vec{\nabla} \times \left(\vec{v} \times \vec{B} \right) + \nu_m \Delta \vec{B}, \tag{16}$$

where $\nu_m = (\mu_0 \sigma)^{-1}$ is called the magnetic diffusivity. Equation (16) together with (10) govern the magnetic field in the MHD approximation. Note however that if (10) is true at $t = 0$, it remains true at any t as shown by taking the divergence of (9).

Knowing $\vec{B}$, we can easily compute the current density from (12) and the electric field from (15). The charge density can be found from $\vec{\nabla} \cdot \vec{j} \approx 0$ which results from (12). Using (8) and (15), we get

$$\rho_e \approx -\epsilon_0 \vec{\nabla} \cdot \left(\vec{v} \times \vec{B} \right). \tag{17}$$

Note that unlike the case of a stationary conductor where ρ_e decays to zero after a transient time of the order of ϵ_0/σ, it is generally non-zero in a moving conductor.

Several approximations have been made when assuming a constant electrical conductivity σ. First, in order to be able to define an electrical conductivity, the collision rate τ^{-1} of electrons with ions should be large compared to the frequency of the fields, i.e. the typical frequency ω of the fluid motion,

$$\omega\tau \ll 1. \tag{18}$$

This is of course verified even in a strongly turbulent liquid metal but not in a rarefied astrophysical plasma.

Second, even in an homogeneous medium the conductivity may vary in space through its dependence on the magnetic field. Indeed, a magnetic field modifies the trajectories of the electrons, and thus the electrical conductivity; this is called the magnetoresistance phenomenon. This can be neglected if the trajectory of an electron is not modified by the magnetic field between two successive collisions, i.e. if the collision rate is very large compared to the Larmor frequency

$$\frac{1}{\tau} \gg \frac{eB}{m}, \tag{19}$$

where e is the charge of the electron and m is its mass. Using the expression of the electrical conductivity, $\sigma = ne^2\tau/m$ gives in the case of a liquid metal an upper limit of thousands of Teslas for the magnetic field. Thus we can safely neglect magnetoresistance.

We have finally to determine the back reaction of the magnetic field on the flow. The electromagnetic force per unit volume is $\rho_e\vec{E} + \vec{j}\times\vec{B}$. Using (17) and $E \sim VB$, we get that the electric force is smaller that the magnetic one by a factor $(V/c)^2$ and we thus neglect it. For a compressible Newtonian flow, we have

$$\frac{\partial\rho}{\partial t} + \vec{\nabla}\cdot(\rho\vec{v}) = 0, \tag{20}$$

where ρ is the fluid density, and

$$\rho\left(\frac{\partial\vec{v}}{\partial t} + (\vec{v}.\vec{\nabla})\vec{v}\right) = -\vec{\nabla}p + \eta\Delta\vec{v} + \left(\zeta + \frac{\eta}{3}\right)\vec{\nabla}(\vec{\nabla}\cdot\vec{v}) + \vec{j}\times\vec{B}, \tag{21}$$

where $p(\vec{r}, t)$ is the pressure field, $\eta = \rho\nu$ is the fluid shear viscosity and ζ is its bulk viscosity.

2.2. *Relation with a two-fluid model*

It may be interesting to determine which terms have been neglected in the MHD approximation compared to a two-fluid hydrodynamic model written for electrons and ions. Conservation of particle numbers gives

$$\frac{\partial n}{\partial t} + \vec{\nabla} \cdot (n\vec{u}) = 0, \tag{22}$$

$$\frac{\partial N}{\partial t} + \vec{\nabla} \cdot (N\vec{U}) = 0, \tag{23}$$

where $n(\vec{r}, t)$ (respectively $N(\vec{r}, t)$) is the density of electrons (respectively ions) of mean velocity $\vec{u}(\vec{r}, t)$ (respectively $\vec{U}(\vec{r}, t)$). Conservation of momentum gives

$$mn\left(\frac{\partial \vec{u}}{\partial t} + (\vec{u}.\vec{\nabla})\vec{u}\right) = -\vec{\nabla}\pi - ne(\vec{E} + \vec{u} \times \vec{B}) + \vec{F}, \tag{24}$$

$$MN\left(\frac{\partial \vec{U}}{\partial t} + (\vec{U}.\vec{\nabla})\vec{U}\right) = -\vec{\nabla}\Pi + Ne(\vec{E} + \vec{U} \times \vec{B}) - \vec{F}, \tag{25}$$

where m (respectively M) is the mass of the electrons (respectively ions), and $\vec{F}$ (respectively $-\vec{F}$) represents the effect of the collisions of the ions on the electrons (respectively of the electrons on the ions). For simplicity, we have assumed that the ions have a charge $+e$ and we do not try to describe viscous forces.

We have $M \gg m$, thus assuming equipartition of energy between electrons and ions gives $MU \gg mu$. Our aim is to find the equations for the fields

$$\rho = NM + nm \approx NM, \tag{26}$$

$$\rho_e = (N - n)e, \tag{27}$$

$$\vec{v} = \frac{1}{\rho}(NM\vec{U} + nm\vec{u}) \approx \vec{U}, \tag{28}$$

$$\vec{j} = e(N\vec{U} - n\vec{u}). \tag{29}$$

Adding (respectively subtracting) (22) and (23) gives the equation of conservation of mass (respectively charge). Adding (24) and (25) gives the

Euler equation for $\vec{v}(\vec{r}, t)$ with the force per unit volume $\rho_e \vec{E} + \vec{j} \times \vec{B}$. Subtracting (24) from (25) gives in the limit of small velocities and taking into account $n \approx N$ and $\vec{v} \approx \vec{U}$

$$\frac{\partial \vec{j}}{\partial t} \approx \frac{e}{m} \vec{\nabla} \pi - \frac{e}{m} \vec{F} + \frac{ne^2}{m} \left(\vec{E} + \vec{v} \times \vec{B} \right) - \frac{e}{m} \vec{j} \times \vec{B}. \qquad (30)$$

In the absence of current, the mean velocities of the ions and the electrons are equal, thus the mean collision force $\vec{F}$ is zero. For a small current density, $\vec{F}$ is proportional to $\vec{j}$ and the electrical conductivity σ is defined by $\sigma \vec{F} = -ne\vec{j}$. This yields

$$\frac{\partial \vec{j}}{\partial t} \approx \frac{e}{m} \vec{\nabla} \pi + \frac{ne^2}{m} \left(\vec{E} + \vec{v} \times \vec{B} - \frac{\vec{j}}{\sigma} \right) - \frac{e}{m} \vec{j} \times \vec{B}. \qquad (31)$$

The terms in parentheses lead to Ohm's law if the others are negligible. We can neglect the first one provided that $\omega \tau \ll 1$ and the last one if $\tau^{-1} \gg eB/m$. We thus recover the conditions (18) and (19) for the validity of the MHD approximation. The last term in equation (31) represents the Hall effect and may be important in some astrophysical plasmas.

2.3. Boundary conditions

Two fields are involved in the MHD equations: the velocity and the magnetic field. Their boundary conditions are of different nature.

For the velocity field, one usually assumes that the fluid velocity at the boundary is equal to the one of the boundary in the case of a viscous fluid. Thus the value of the fluid velocity is determined locally at the boundary.

The problem is not so simple for the magnetic field because its value must be calculated in the whole space. In a laboratory experiment, the flow can be bounded by a shell made of a metal with an electrical conductivity and a magnetic permeability μ different from the ones of the fluid. The boundary conditions are derived from the MHD equations. Equation (10) implies that the normal component of the magnetic field is continuous. From the definition of the magnetic permeability, we have $\vec{\nabla} \times \vec{H} = \vec{j}$, with $\vec{B} = \mu \vec{H}$, such that the tangential part of $\vec{B}/\mu$ is continuous. Equation (9), implies that the tangential part of $\vec{E} = \nu_m \vec{\nabla} \times \vec{B} - \vec{v} \times \vec{B}$ is continuous. Values of the field in the different media are related by these boundary conditions. Outside the fluid container or outside an astrophysical object, the field in vacuum is solution of $\vec{\nabla} \cdot \vec{B} = 0$ and $\vec{\nabla} \times \vec{B} = 0$. It can be calculated using a scalar potential V such that $\vec{B} = -\vec{\nabla} V$ and $\Delta V = 0$. Then, the boundary conditions on the magnetic field at the solid-vacuum interface relates the fields in the internal and external media.

The most common configuration studied in astrophysics or geophysics consists of an electrically conducting fluid in a spherical domain surrounded by an insulating medium. The spherical geometry leads to a simple solution for the outer magnetic field. Analytical dynamo examples often involve more artificial configurations: fluid within a solid medium with the same electrical conductivity extending to infinity (Ponomarenko's dynamo), periodic flow and thus periodic boundary conditions (Roberts' dynamo). In these cases, one should be careful in order to avoid dynamo generation from an inappropriate choice of boundary conditions [5]. Solid boundaries of infinite electrical conductivity have been sometimes considered. For some particular flows, it has been shown that this configuration is more efficient for dynamo generation than the similar one with insulating boundaries [13]. This is a very interesting observation for laboratory experiments. Although boundaries of large electrical conductivity compared to the one of the fluid are not realistic, a factor of order 5 may be obtained with liquid sodium inside a container made of copper. It is not known whether there exists an optimum conductivity ratio for dynamo action. It has been observed recently that it may be also advantageous to have boundaries with the same electrical conductivity as the one of the liquid metal. This is easy to implement both in experiments (by keeping the liquid metal at rest in the outer region [37]) and in numerical simulations. However, the resulting threshold shift may have both signs [14]. It is also possible to optimize dynamo generation using boundaries made of high magnetic permeability metal which tend to canalize the field lines. This has been shown with simple analytical dynamos [15] but has never been tried in experiments. The effect of boundary conditions on the dynamo threshold still deserves a lot of studies but, unfortunately, it may depend on each flow configuration thus preventing the existence of general rules.

2.4. *Relevant dimensionless numbers*

We will mostly consider flows in liquid metals at velocities much less than sound velocity and assume incompressibility. We thus have the following parameters in the equations for the magnetic and velocity fields: $\mu_0\sigma$, ρ and ν. Assuming that the flow has a typical length scale L and a velocity scale V, we have two independent dimensionless parameters. We can choose the typical ratios of the advective versus diffusive terms in the equations for transport of momentum and magnetic field. The two dimensionless numbers are thus the Reynolds number,

$$Re = \frac{VL}{\nu}, \qquad (32)$$

and the magnetic Reynolds number,

$$R_m = \mu_0 \sigma V L. \tag{33}$$

Using L, L/V, V, ρV^2 and $\sqrt{\mu_0 \rho} V$ as units for length, time, velocity, pressure and magnetic field respectively, we can write the MHD equations in dimensionless form

$$\vec{\nabla} \cdot \vec{B} = 0, \tag{34}$$

$$\frac{\partial \vec{B}}{\partial t} = \vec{\nabla} \times (\vec{v} \times \vec{B}) + \frac{1}{R_m} \Delta \vec{B}, \tag{35}$$

$$\vec{\nabla} \cdot \vec{v} = 0, \tag{36}$$

$$\frac{\partial \vec{v}}{\partial t} + (\vec{v}.\vec{\nabla})\vec{v} = -\vec{\nabla}\left(p + \frac{B^2}{2}\right) + \frac{1}{Re}\Delta \vec{v} + (\vec{B} \cdot \vec{\nabla})\vec{B}. \tag{37}$$

We have used equation (12) in the expression of the Laplace force in equation (37). We emphasize that, although we have not used new notations, all the fields in the above equations are dimensionless. Note also that other dimensionless numbers should be considered if the flow involves more than one length scale or velocity scale and in the case of particular electric or magnetic boundary conditions. We will consider some of these problems later.

The kinematic dynamo problem consists of solving equations (34, 35) for a given velocity field $\vec{v}(\vec{r}, t)$. The problem is linear in $\vec{B}(\vec{r}, t)$ and one has to find the growth rate $\eta(R_m)$ of the eigenmodes of the magnetic field. If $R_m \to 0$, Joule dissipation is dominant and after rescaling time in (35) we get a diffusion equation for $\vec{B}(\vec{r}, t)$, thus $\vec{B}(\vec{r}, t) \to 0$ for $t \to \infty$. The dynamo threshold corresponds to the value R_{mc} of R_m for which the growth rate of one eigenmode first vanishes and then changes sign. The solution $B = 0$ of equations (34, 35) thus becomes unstable. For some particular velocity fields, this may not occur for any value of R_m (see the section on "antidynamo theorems"). For the others, the dynamo instability occurs for a large enough value of R_m for which the effect of the advective term in (35) overcomes Joule dissipation. Another interesting mathematical problem concerns the behavior of the growth rate in the limit $R_m \to \infty$. For some fluid dynamos it stays finite, whereas it vanishes for others. This is of little interest for present laboratory experiments but may have important implications in astrophysics. Going back to dimensional variables, the question is to determine whether the growth of the field generated by a dynamo occurs on the convective time scale L/V or on the diffusive time

scale $\mu_0 \sigma L^2$ which is R_m times larger. The dynamo is called "fast" in the first case and "slow" in the second one. R_m being huge for astrophysical flows, a slow dynamo may have had not enough time to operate and thus be of little interest.

It is possible to compare the mean drift velocity of the electrons to the one of the ions in the limit of validity of the MHD approximation given by equation (19). Using this condition together with the expression of the electrical conductivity, we can write

$$V \gg R_m \frac{j}{ne} \,. \tag{38}$$

This shows that, even for the highest magnetic fields or currents within the range of validity of the MHD approximation, the fluid velocity is large compared to the drift velocity of the electrons relative to the ions provided that R_m is large enough.

The fluid dynamo problem is much more difficult when the velocity field is not fixed but should be found by solving the full set of equations (34, 35, 36, 37). This is called the dynamic dynamo problem, often associated with the effect of the back reaction of the Laplace force on the flow in equation (37). We emphasize that this is not the only additional difficulty. Open questions already exist at the level of the dynamo onset for which there is no effect of the Laplace force. The dynamo onset corresponds to a curve $R_{mc} = R_{mc}(Re)$ in the $Re - R_m$ plane. This reflects the fact that the geometry of the velocity field is no longer fixed but may depend on the fluid viscosity ν and on the typical velocity V and length scale L determined for instance by the motion of solid boundaries that drive the flow. Depending on the value of the Reynolds number, the flow may be more or less turbulent and this may affect the value of the dynamo threshold. Little is known and understood about this effect i.e. on the behavior of $R_{mc}(Re)$ in the limit $Re \to \infty$. This is however the realistic limit for all laboratory fluid dynamos. Indeed, the magnetic Prandtl number

$$P_m = \frac{R_m}{Re} = \mu_0 \sigma \nu \tag{39}$$

is less that 10^{-5} for all liquid metals. Since we expect the dynamo threshold for large enough R_m, then Re is at least of the order of a million and the flow is fully turbulent. We will discuss the effect of turbulence on dynamo threshold in section 6.

Another open problem concerns the saturation value of the magnetic field generated by a fluid dynamo. Above threshold, the Laplace force modifies the velocity field thus affecting the induction equation (35). This

should in principle saturate the growth of the amplitude of the magnetic field. Dimensional analysis only gives

$$B^2 = \mu_0 \rho V^2 \, f(R_m, Re), \tag{40}$$

where f is a priori an arbitrary function of R_m and Re. We will discuss some scaling laws for f in section 7.

2.5. Some limits of the MHD equations

If we can neglect Joule dissipation, we can take the limit $\sigma \to \infty$ i.e. $\nu_m \to 0$ in the induction equation (16). Even if the fluid is compressible, simple manipulations using (20,16) give

$$\frac{D}{Dt}\left(\frac{\vec{B}}{\rho}\right) = \frac{\partial}{\partial t}\left(\frac{\vec{B}}{\rho}\right) + \left(\vec{v}\cdot\vec{\nabla}\right)\left(\frac{\vec{B}}{\rho}\right) = \left(\frac{\vec{B}}{\rho}\cdot\vec{\nabla}\right)\vec{v}, \tag{41}$$

showing that $\vec{B}/\rho$ obeys the same equation as a fluid element $\delta\vec{l}$ advected by the flow. In the limit of infinite conductivity, the magnetic field lines move with the fluid elements. They are said to be frozen in the flow. Using Lagrangian coordinates, we can write formally the Cauchy solution for the magnetic field [7]. $\vec{B}/\rho \propto \delta\vec{l}$ gives the scaling $B \propto \rho^{2/3}$ that we have obtained in section 1 for an isotropic compression when we mentioned the relict field hypothesis.

The validity of the infinite conductivity limit requires that one considers the system on time scales small compared to the characteristic dissipation time due to Joule effect. It is thus of little interest for the dynamo problem for which one should show that the magnetic field can be maintained by the flow against Joule dissipation. It has been used however to study various MHD problems, for instance Alfven waves in the presence of an externally applied magnetic field [16].

The opposite limit is the one of small R_m. Of course, no interesting MHD effect happens in the absence of an externally applied magnetic field since the $B = 0$ solution is stable. In the presence of an externally applied magnetic field $\vec{B}_0$, electric currents are generated by the flow and affect it through the Laplace force. If $\vec{B}_0$ is homogeneous, the relevant additional dimensionless number is the interaction parameter, which measures the order of magnitude of the Laplace force compared to the pressure force. Writing $\vec{B} = \vec{B}_0 + \vec{b}$ where $\vec{b}(\vec{r}, t)$ is the magnetic field generated by the induced currents, we get from the induction equation (16) at leading order in R_m

$$\left(\vec{B}_0 \cdot \vec{\nabla}\right)\vec{v} + \nu_m \Delta\vec{b} \approx 0. \tag{42}$$

Thus

$$| \left(\vec{B} \cdot \vec{\nabla} \right) \vec{B}| = | \left(\vec{B}_0 \cdot \vec{\nabla} \right) \vec{b}| \sim \mu_0 \sigma V B_0^2. \tag{43}$$

Dividing by the order of magnitude of the pressure gradient gives the interaction parameter

$$N = \frac{\sigma L B_0^2}{\rho V}. \tag{44}$$

We can also define the Chandrasekhar number, $Q = NRe$, that represents the ratio of the Laplace force to the viscous force. The main effect of $\vec{B}_0$ is to inhibit velocity gradients along its direction and thus to tend to make the flow two-dimensional [17,18]. However, the effect of $\vec{B}_0$ is not always a stabilizing one, in particular in rotating fluids [19,20].

3. Advection and diffusion of a passive vector

We will discuss some simple solutions of the MHD equations showing some elementary effects due to the advection of the magnetic field by the flow of an electrically conducting fluid: accelerated diffusion, local amplification, effect of a shear, of differential rotation, expulsion of a transverse field from a rotating flow.

3.1. *More or less useful analogies*

The formal resemblance of the induction equation

$$\frac{\partial \vec{B}}{\partial t} = \vec{\nabla} \times \left(\vec{v} \times \vec{B} \right) + \nu_m \Delta \vec{B}, \tag{45}$$

to the equation governing the vorticity has been first pointed out by Elsasser [28]. It may be however a misleading analogy because equation (45) is linear in $\vec{B}$ for a given velocity field, whereas the similar equation for $\vec{\omega}$ is nonlinear since $\vec{\omega} = \vec{\nabla} \times \vec{v}$ [7]. For the dynamic dynamo problem, $\vec{B}$ is coupled to $\vec{v}$ through the Laplace force in the Navier-Stokes equation and there is no analogy left. We also emphasize that the boundary conditions for $\vec{\omega}$ and $\vec{B}$ are different: vorticity is usually generated at the boundaries and advected in the bulk of the flow. This is not the generation mechanism for the magnetic field we are looking for when studying the dynamo problem.

For an incompressible fluid, equation (45) can be written in the form

$$\frac{\partial \vec{B}}{\partial t} + \left(\vec{v} \cdot \vec{\nabla} \right) \vec{B} = \left(\vec{B} \cdot \vec{\nabla} \right) \vec{v} + \nu_m \Delta \vec{B}, \tag{46}$$

and thus is similar to the equation governing the advection of a passive scalar, for instance a concentration field $C(\vec{r}, t)$ by a given flow $\vec{v}$,

$$\frac{\partial C}{\partial t} + \vec{v} \cdot \vec{\nabla} C = D\Delta C, \tag{47}$$

provided that $(\vec{B} \cdot \vec{\nabla})\vec{v} = 0$. Therefore we expect that the effects observed with passive scalar advection, and in particular accelerated diffusion by a velocity field, also occur with the advection of a magnetic field. However, the dynamo effect, when it occurs, is clearly due to the additional term $(\vec{B} \cdot \vec{\nabla})\vec{v}$. Indeed, multiplying (47) and integrating on the whole volume Ω of the flow gives

$$\frac{1}{2}\frac{d}{dt}\int_\Omega C^2 \, d^3x = -D\int_\Omega \left(\vec{\nabla}C\right)^2 d^3x. \tag{48}$$

We have assumed that the flow is bounded by an impermeable surface on which the normal velocity and the normal concentration gradient vanish. Taking the average of equation (47) on Ω shows that the spatial mean of the concentration $\langle C \rangle$ is constant, an obvious result from mass conservation. Thus, equation (48) shows that the variance of the concentration, $\langle C^2 \rangle - \langle C \rangle^2$ decreases in time until the concentration field becomes homogeneous. Although not explicitly apparent, the effect of the velocity field in (48) is to generate large concentration gradients and thus to accelerate homogenization. Similarly, it is clear that the dynamo effect, i.e. an increase of the magnetic energy, cannot occur if the term $(\vec{B} \cdot \vec{\nabla})\vec{v}$ vanishes.

3.2. *Accelerated diffusion*

The simplest way to recover the effects of passive scalar advection for the magnetic field, is to consider geometrical configurations for which $(\vec{B} \cdot \vec{\nabla})\vec{v}$ vanishes. This occurs for instance when the velocity field is two-dimensional, $\vec{v} = (u(x, y, z, t), v(x, y, z, t), 0)$ and the magnetic field perpendicular to $\vec{v}$, $\vec{B} = B(x, y, t)\,\hat{z}$, where $\hat{z}$ is the unit vector along the z-axis. $B(x, y, t)$ obeys the advection-diffusion equation (47).

3.2.1. *Effect of a shear*

We first consider the effect of a shear flow, $\vec{v} = (\alpha y, 0, 0)$ on a magnetic field of the form $B(x, y, t = 0) = B_0 \sin k_0 x$. We thus have from (47)

$$\frac{\partial B}{\partial t} + \alpha y \frac{\partial B}{\partial x} = \nu_m \left(\frac{\partial^2 B}{\partial x^2} + \frac{\partial^2 B}{\partial y^2}\right). \tag{49}$$

In the limit of infinite conductivity, $\nu_m = 0$, the field is just advected by the flow

$$B_{\text{adv}} = B_0 \sin k_0(x - \alpha y t). \tag{50}$$

For finite ν_m, we look for a solution in the form $B(x, y, t) = f(t)B_{\text{adv}}$ and get from (49)

$$\dot{f} = -\nu_m k_0^2 (1 + \alpha^2 t^2) f. \tag{51}$$

We thus have

$$B(x, y, t) = B_0 \sin k_0(x - \alpha y t) \, \exp\left(-\nu_m k_0^2 (t + \frac{\alpha^2}{3} t^3)\right). \tag{52}$$

With equation (48) in mind, we compute $\langle (\vec{\nabla} B)^2 \rangle$

$$\langle (\vec{\nabla} B)^2 \rangle = \frac{1}{2} B_0^2 k_0^2 \left(1 + \alpha^2 t^2\right) \exp\left(-2\nu_m k_0^2 (t + \frac{\alpha^2}{3} t^3)\right). \tag{53}$$

$\langle (\vec{\nabla} B)^2 \rangle$ begins to increase as in the case without diffusion. When large enough gradients have been generated by the advection of the magnetic field by the shear flow, Joule dissipation becomes important and $\langle (\vec{\nabla} B)^2 \rangle$ decreases to 0. For ν_m small, the characteristic time for which $\langle (\vec{\nabla} B)^2 \rangle$ begins to decrease is

$$\tau_{\text{shear}} \propto \left(\nu_m k_0^2 \alpha^2\right)^{-\frac{1}{3}}. \tag{54}$$

τ_{shear} is the effective diffusion time by the shear flow and should be compared to the diffusion time in the absence of flow $\tau_d = (\nu_m k_0^2)^{-1}$ which is much longer if ν_m is small.

3.2.2. Effect of a strain

We now consider the effect of a flow with a uniform rate of strain, $\vec{v} = (\alpha x, -\alpha y, 0)$. We have to solve

$$\frac{\partial B}{\partial t} + \alpha x \frac{\partial B}{\partial x} - \alpha y \frac{\partial B}{\partial y} = \nu_m \left(\frac{\partial^2 B}{\partial x^2} + \frac{\partial^2 B}{\partial y^2}\right). \tag{55}$$

We look for a solution of the form $B(x, y, t) = B_0 f(t) \sin k(t)x$ and get [7]

$$k(t) = k_0 \, e^{-\alpha t}, \tag{56}$$

$$B(x, y, t) = B_0 \exp\left[\frac{\nu_m k_0^2}{2\alpha} \left(e^{-2\alpha t} - 1)\right)\right] \sin k(t)x. \tag{57}$$

If $\alpha < 0$, the flow generates large gradients of B and this strongly increases Joule dissipation, thus leading to an effective diffusion time

$$\tau_{\text{strain}} \propto \frac{1}{\alpha} Log\left(\frac{\alpha}{\nu_m k_0^2}\right). \tag{58}$$

For ν_m small, τ_{strain} is much smaller than τ_{shear}, thus showing that mixing is more efficient than with a shear flow. This is clearly due to the fact that large gradients are generated more quickly within the regions of large strain.

3.3. *Local amplification*

Another simple configuration consists of a magnetic field, $\vec{B} = (B_x(x,y,t), B_y(x,y,t), 0)$, in the plane of a two-dimensional flow, $\vec{v} = (v_x(x,y,t), v_y(x,y,t), 0)$. It is convenient to consider the equation governing the vector potential $\vec{A}$ with $\vec{B} = \vec{\nabla} \times \vec{A}$. We get from equation (45)

$$\frac{\partial \vec{A}}{\partial t} = \vec{v} \times \left(\vec{\nabla} \times \vec{A}\right) - \vec{\nabla}\phi + \nu_m \Delta \vec{A}, \tag{59}$$

where $\phi(x,y,z,t)$ is the scalar potential.

For a two-dimensional magnetic field, $\vec{B} = \vec{\nabla} \times (A\hat{z}) = \vec{\nabla} A \times \hat{z} = (\partial A/\partial y, -\partial A/\partial x, 0)$, we have

$$\frac{\partial A}{\partial t} + \vec{v} \cdot \vec{\nabla} A = \nu_m \Delta A, \tag{60}$$

thus A obeys an advection-diffusion equation. Consequently, we do not expect new effects compared to the passive scalar advection. However, it is interesting to discuss some consequences of equation (60) in terms of the magnetic field.

3.3.1. *Effect of a shear*

We first consider the effect of a shear flow $\vec{v} = (\alpha y, 0, 0)$ on an externally applied transverse magnetic field $\vec{B}_0 = (0, B_0, 0)$. The equation governing the vector potential $A\hat{z}$ is

$$\frac{\partial A}{\partial t} + \alpha y \frac{\partial A}{\partial x} = \nu_m \Delta A. \tag{61}$$

If we consider the behavior of the magnetic field on a short time scale after turning on the flow, we can neglect diffusion and we get the solution, $A(x,y,t) = -B_0(x - \alpha y t)$, thus $\vec{B} = (B_0\alpha t, B_0, 0)$. We thus observe that a magnetic field along the axis of the shear is induced. We look for a

stationary solution of equation (61) in the form $A(x, y) = -B_0 x + f(y)$ and get for the magnetic field $\vec{B} = \left(B_0 \alpha y^2 / 2\nu_m, B_0, 0\right)$. The solution goes to infinity because the applied magnetic field and the velocity field both extend to infinity.

If we consider a localized jet around the x-axis, of the form $\vec{v} = \left(v_0 / \cosh^2 ky, 0, 0\right)$, we get $\vec{B} = (-B_0 R_m \tanh ky, B_0, 0)$, where $R_m = v_0 / k\nu_m$. The induced field is constant for $y \to \pm\infty$ because the jet is infinite along the x-axis. We thus find that at large R_m, the magnetic field tends to become aligned with the shear flow. This can be understood very easily by looking at the current induced by the interaction of the externally applied magnetic field with the velocity field.

3.3.2. *Effect of a strain*

We next consider the effect of a flow with a uniform rate of strain, $\vec{v} = (\alpha x, -\alpha y, 0)$, on a magnetic field along the x-axis, and thus depending only on y and t $(\alpha > 0)$. We have to solve

$$\frac{\partial A}{\partial t} - \alpha y \frac{\partial A}{\partial y} = \nu_m \frac{\partial^2 A}{\partial y^2}. \tag{62}$$

We thus get for the stationary solution of the magnetic field, $\vec{B} = B_0 \exp\left(-\alpha y^2 / 2\nu_m\right) \hat{x}$. This solution is similar to the one of the Burgers vortex for vorticity amplified by strain. The magnetic field is concentrated on a typical length scale $\sqrt{\nu_m / \alpha}$. A magnetic tube of length l along the x-axis becomes elongated along x and thus thinner along y, when it is advected toward the x-axis; thus the magnetic field is amplified in order to have flux conservation. We can indeed check that the total magnetic flux is conserved [7]. Let us emphasize that we do not have here any dynamo effect but just local amplification of an existing magnetic field by the flow.

3.4. *Expulsion of a transverse magnetic field from a rotating eddy*

We study the effect of a rotating eddy on a transverse magnetic field $\vec{B}_0 = B_0 \hat{y}$ as sketched in Figure 3. The eddy of radius R is infinite in the axial direction $\hat{x}$ and rotates at an angular velocity ω. The results do not depend on the electrical conductivity of the external medium (conductor or insulating).

Writing $\vec{B} = \vec{B}_0 + \vec{b}$, the stationary induced magnetic field is solution of the equation

$$\nu_m \Delta \vec{b} + \nabla \times (\vec{v} \times \vec{b}) = -\nabla \times (\vec{v} \times \vec{B}_0). \tag{63}$$
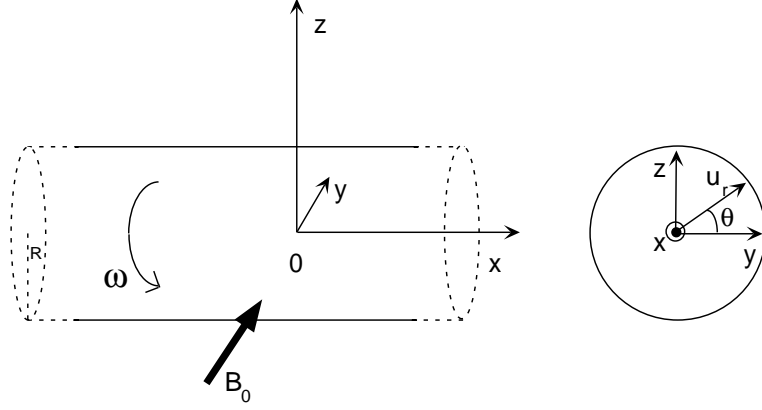
Figure 3. Rotating eddy submitted to a transverse magnetic field.

In the limit of low velocity, $b \ll B_0$ and we have to solve

$$\nu_m \, \Delta \, \vec{b} \approx -\nabla \times (\vec{v} \times \vec{B}_0) \,. \tag{64}$$

Using cylindrical coordinates ($\hat{r} = \cos\theta \hat{y} + \sin\theta \hat{z}$), we obtain for $r \leq R$

$$b_r = -\frac{B_0 \, \omega \, R^2}{8 \, \nu_m} \left(\left(\frac{r}{R} \right)^2 - 2 \right) \sin\theta \,,$$

$$b_\theta = \frac{B_0 \, \omega \, R^2}{8 \, \nu_m} \left(2 - 3 \left(\frac{r}{R} \right)^2 \right) \cos\theta \,,$$

$$b_x = 0 \,. \tag{65}$$

This field is generated by the interaction between the rotating eddy and the applied magnetic field $\vec{B}_0$ which creates a current $\vec{j}_1$ and a magnetic field $\vec{b}_1$ as sketched in Figure (4 a). With the description of this "one-step" mechanism, one can understand the linear dependence of the field in ω.

At higher velocity, terms of higher order must be taken into account. The solution of equation (63) is given in terms of the Bessel function $I(n, x)$ [21]

$$b_r = B_0 \, Re \left((\frac{I(0, q \, r)}{I(0, q \, R)} - \frac{I(2, q \, r)}{I(0, q \, R)} - 1) \exp\left(i \, \theta \right) \right) \,,$$

$$b_\theta = B_0 \, Re \left((\frac{I(2, q \, r)}{I(0, q \, R)} + \frac{I(0, q \, r)}{I(0, q \, R)} - 1) \exp\left(i \, (\theta + \pi/2) \right) \right) \,,$$

$$b_x = 0 \,, \tag{66}$$

where $q = \exp(i\pi/4)\sqrt{\frac{\omega}{\nu_m}}$. Expanding this result in successive powers of the angular velocity gives

$$
\begin{aligned}
b_r = &-\frac{B_0\,\omega\,R^2}{8\,\nu_m}\left(\left(\frac{r}{R}\right)^2 - 2\right)\sin\theta \\
&+ \frac{B_0\,\omega^2\,R^4}{\nu_m^2}\left(-\frac{\left(\frac{r}{R}\right)^4}{192} + \frac{\left(\frac{r}{R}\right)^2}{32} - \frac{3}{64}\right)\cos\theta\,, \\
b_\theta = &\frac{B_0\,\omega\,R^2}{8\,\nu_m}\left(2 - 3\left(\frac{r}{R}\right)^2\right)\cos\theta \\
&- \frac{B_0\,\omega^2\,R^4}{\nu_m^2}\left(\frac{5\left(\frac{r}{R}\right)^4}{192} - \frac{3\left(\frac{r}{R}\right)^2}{32} + \frac{3}{64}\right)\sin\theta\,, \\
b_x = &0\,.
\end{aligned}
\tag{67}
$$

The term linear in ω is the one previously calculated. The quadratic term results from the interaction of the induced magnetic field b_1 with the velocity field as sketched in Figure (4 b). In that sense, this is a "two-step" mechanism and since b_1 is linear in ω, b_2 is quadratic.

These are the first steps of the mechanism of expulsion of the transverse magnetic field. At very high velocity, the field enters the eddy only in a small diffusive layer of length $\sqrt{\nu_m/\omega}$. This corresponds to the usual skin effect as can be understood in the frame of the rotating eddy where the applied magnetic field is oscillatory.

In the case of a liquid metal in rotation in a cylindrical container, the velocity field vanishes at the boundaries and solid body rotation is thus achieved only in the bulk. Then, a transverse magnetic field is expelled from the bulk but becomes more intense near the boundaries as shown by experiments made in liquid gallium [22].

3.5. *Effect of differential rotation and the Herzenberg dynamo*

We have already shown that a shear flow generates a magnetic field component parallel to the shear from a perpendicularly applied one. In other words, field lines tend to become aligned along the shear and the field amplitude is enhanced if the shear is strong enough. In geophysical and astrophysical fluid dynamics, very common flows with shear are axisymmetric flows which involve differential rotation. For such flows, a toroidal field is generated from an applied poloidal one. This effect is called the ω-effect and is very similar to the effect of a shear presented above. We sketch this mechanism in Figure 5 in the limit of zero magnetic viscosity ("frozen
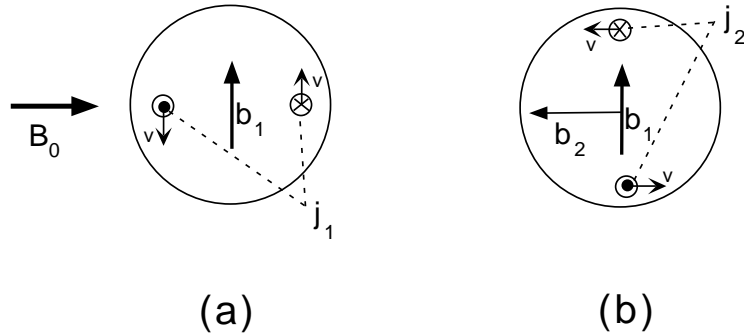
Figure 4. Induction mechanism for a rotating eddy submitted to a transverse magnetic field. (a): the interaction of B_0 with the velocity v creates a current j_1 and an induced field b_1. (b): the interaction between b_1 and v creates a current j_2 and an induced field b_2.

field"). If the flow is in solid body rotation, any meridional field is advected by the flow and its magnitude remains constant. If the flow involves differential rotation, the frozen magnetic field tends to become aligned with the shear and an azimuthal field is thus generated. This is the mechanism of the ω-effect which transforms a meridional field into an azimuthal one. If B_0 is the field amplitude along the z-axis, the azimuthal component is generated by the term $B_0\,\partial\vec{v}_\theta/\partial z$ of the induction equation.

Simple rotor dynamos are based on this mechanism. The first model was presented by Herzenberg [23]. It consists of two rotating spheres in electrical contact with a conducting medium at rest. A similar model, made with rotating cylinders instead of spheres, was built by Lowes and Wilkinson and provided the first experimental demonstration of an homogeneous dynamo [24]. The dynamo mechanism is sketched in Figure 6. A magnetic field perturbation along the axis of cylinder 1 generates a toroidal field via the ω-effect. If the axis of the cylinders are not parallel, any toroidal field for cylinder 1 has a poloidal component for cylinder 2. Then, cylinder 2 creates a toroidal field via the ω-effect. This toroidal field has a poloidal component for cylinder 1, and thus may enhanced the initial perturbation provided the rotation rates are strong enough. It should be also noted that one of the two steps has a vanishing contribution if the vector $\vec{d}$ joining the centers of the two cylinders, is parallel to one of the two rotation vectors $\vec{\Omega}_i$ of the cylinders. Thus, dynamo action also requires $\vec{\Omega}_1\cdot(\vec{\Omega}_2\times\vec{d})\neq 0$, which can be understood as a condition on the helicity of the "flow".

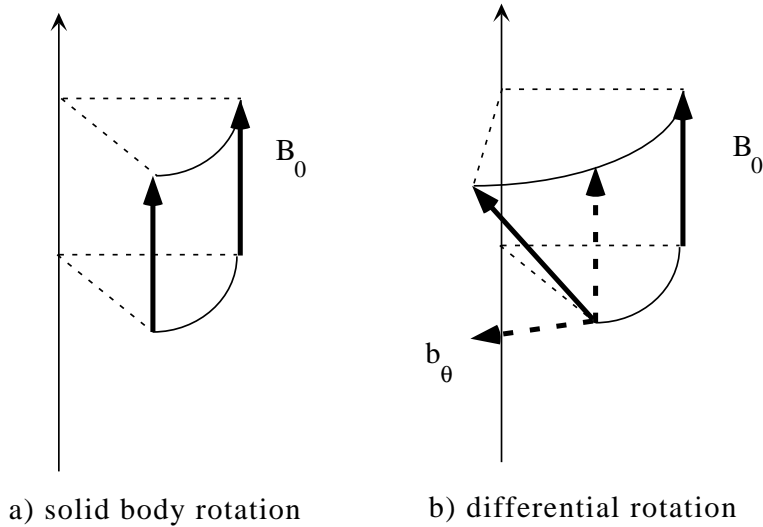a) solid body rotation   b) differential rotation

Figure 5.   (a) A magnetic field frozen in the fluid is advected without being modified by solid body rotation. (b) In the case of differential rotation, the field lines become aligned with the shear. This generates an azimuthal field component.

4. Necessary conditions for dynamo action

We will consider the equation governing the magnetic energy and use it to find necessary conditions for an increase of the magnetic energy from mechanical work. In particular we will discuss the importance of the flow geometry and review some configurations for which the dynamo action does not occur.

4.1. *Magnetic energy*

We consider the flow of an electrically conducting fluid in a volume Ω inside a surface S surrounded by a motionless insulator occupying the rest of space. We assume that there are no sources of field outside Ω, thus

$$E = O(r^{-2}),\ B = O(r^{-3}) \text{ as } r \to \infty. \tag{68}$$

From equation (9), we get for the evolution of the magnetic energy, E_M,

$$\frac{dE_M}{dt} = \frac{d}{dt} \int \frac{B^2}{2\mu_0}\, d^3x = \int \frac{\vec{B}}{\mu_0} \frac{\partial \vec{B}}{\partial t}\, d^3x = - \int \frac{\vec{B}}{\mu_0} \vec{\nabla} \times \vec{E}\, d^3x. \tag{69}$$

Using $\vec{\nabla} \cdot (\vec{B} \times \vec{E}) = -\vec{B} \cdot (\vec{\nabla} \times \vec{E}) + \vec{E} \cdot (\vec{\nabla} \times \vec{B})$ and taking into account that $|\vec{E} \times \vec{B}| = O(r^{-5})$ as $r \to \infty$ such that we have no contribution from
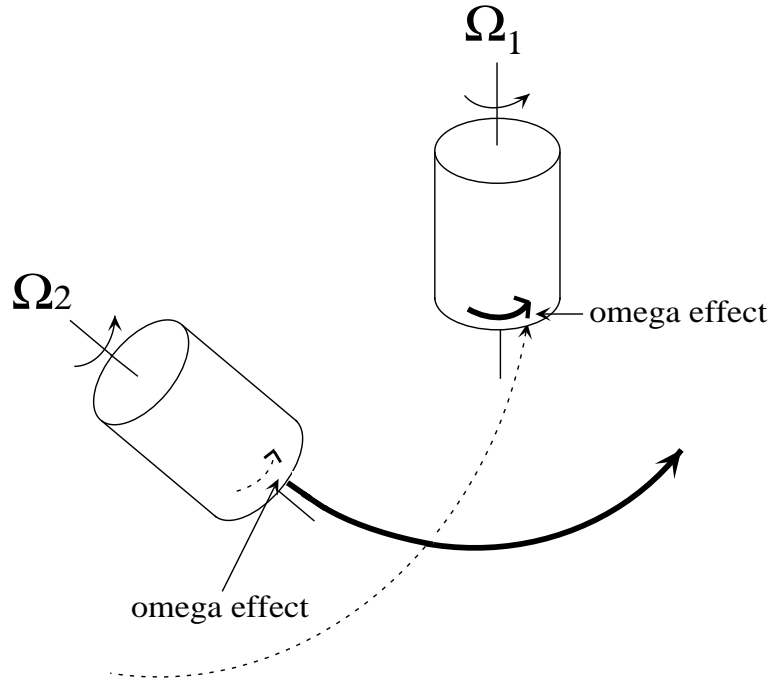
Figure 6. Rotating cylinders in electrical contact with an electrically conducting medium at rest. The toroidal field of each cylinder has a non-zero component along the axis of the other one. Thus each toroidal field may be generated by the other one through the ω-effect.

its surface integral, we get

$$\frac{dE_M}{dt} = -\int_\Omega \vec{E} \cdot \vec{j}\, d^3x.$$ (70)

Then, Ohm's law (15) gives

$$\frac{dE_M}{dt} = \int_\Omega (\vec{v} \times \vec{B}) \cdot \vec{j}\, d^3x - \int_\Omega \frac{\vec{j}^2}{\sigma}\, d^3x.$$ (71)

The last term of equation (71) represents Joule dissipation, whereas the first term of the right hand side describes energy transfer from the velocity field and may lead to an increase of the magnetic energy if it overcomes Joule dissipation.

Using the Cauchy-Schwarz inequality, we obtain

$$\left| \int_\Omega \vec{v} \cdot (\vec{B} \times (\vec{\nabla} \times \vec{B})) d^3x \right| \leq V_M \int_\Omega |\vec{B}||\vec{\nabla} \times \vec{B}| \, d^3x$$

$$\leq V_M \left[\int B^2 \, d^3x \right]^{\frac{1}{2}} \left[\int_\Omega (\vec{\nabla} \times \vec{B})^2 d^3x \right]^{\frac{1}{2}} \quad (72)$$

where V_M is the maximum of $|\vec{v}|$ on Ω. Defining

$$\frac{1}{H^2} \equiv \min \left[\frac{\int_\Omega (\vec{\nabla} \times \vec{B})^2 \, d^3x}{\int B^2 \, d^3x} \right], \quad (73)$$

where the minimum is taken on all possible admissible magnetic fields (solenoidal, irrotational outside Ω, $O(r^{-3})$ at infinity and satisfying the appropriate boundary conditions on S), we get

$$\frac{dE_M}{dt} \leq \frac{1}{\mu_0^2 \sigma} (\mu_0 \sigma V_M H - 1) \int_\Omega (\vec{\nabla} \times \vec{B})^2 \, d^3x. \quad (74)$$

A necessary condition for dynamo action is thus [2]

$$\mu_0 \sigma V_M H \geq 1. \quad (75)$$

A second condition can be obtained if the flow is incompressible. Using $\vec{B} \times (\vec{\nabla} \times \vec{B}) = \vec{\nabla}(B^2/2) - (\vec{B} \cdot \vec{\nabla})\vec{B}$, we obtain

$$\int_\Omega \vec{v} \cdot (\vec{B} \times (\vec{\nabla} \times \vec{B})) \, d^3x = \int_S \frac{B^2}{2} \vec{v} \cdot \hat{n} dS - \int_\Omega \vec{v} \cdot (\vec{B} \cdot \vec{\nabla})\vec{B} \, d^3x. \quad (76)$$

On the right hand side, the incompressibility condition and the divergence theorem have been used to transform the first term which vanishes because $\vec{v} = 0$ on S. Using $\vec{\nabla} \cdot \vec{B} = 0$ and integrating by parts, we have for the second term in tensor notations

$$\int_\Omega v_i B_j \partial_j B_i \, d^3x = \int_\Omega v_i \partial_j (B_i B_j) \, d^3x$$

$$= \int_S B_i B_j v_i n_j dS - \int_\Omega B_i B_j \partial_j v_i \, d^3x, \quad (77)$$

where the surface integral again vanishes because $\vec{v} = 0$ on S. Thus,

$$\frac{dE_M}{dt} = \frac{1}{2\mu_0} \int_\Omega B_i B_j \left(\partial_j v_i + \partial_i v_j \right) \, d^3x - \int_\Omega \frac{\vec{j}^2}{\sigma} \, d^3x, \quad (78)$$

that can be also found directly by multiplying equation (46) by $\vec{B}$ and integrating over space. It is interesting to compare this second form of the evolution equation for the magnetic energy to the first one (71). In (78), the term describing energy transfer from the velocity field is quadratic in B_i and

involves the derivatives of the velocity field whereas in (71) it involves the velocity field itself times the magnetic field and its space derivatives. Consequently, a second necessary condition for dynamo action can be obtained from (78). Let Λ_M be the maximum eigenvalue of the tensor $(\partial_j v_i + \partial_i v_j)/2$ ($\Lambda_M > 0$ for non vanishing velocity fields). We have

$$\frac{1}{2}\int_\Omega B_i B_j \left(\partial_j v_i + \partial_i v_j\right) d^3 x \leq \Lambda_M \int B^2 d^3 x$$

$$\leq \Lambda_M H^2 \int_\Omega (\vec\nabla \times \vec B)^2 d^3 x, \qquad (79)$$

and consequently

$$\frac{dE_M}{dt} \leq \frac{1}{\mu_0^2 \sigma}(\mu_0 \sigma \Lambda_M H^2 - 1)\int_\Omega (\vec\nabla \times \vec B)^2 d^3 x. \qquad (80)$$

A second necessary condition for dynamo action is thus [25]

$$\mu_0 \sigma \Lambda_M H^2 \geq 1. \qquad (81)$$

4.2. *The critical magnetic Reynolds number*

The above necessary conditions imply that for $\mu_0 \sigma$ fixed, H, Λ_M and V_M should be large enough. The condition on H is easy to understand. H is the typical lengthscale related to the magnetic field gradients and should be as large as possible in order to minimize Joule dissipation. It is less obvious to understand why we have apparently two independent constraints to make the dynamo capability of the term $\vec\nabla \times (\vec v \times \vec B)$ in equation (45) large enough: Λ_M large or V_M large. Are they independent ? At first sight, Λ_M is related to the flow gradients whereas V_M is an absolute velocity magnitude. This is not completely correct because equation (45) is invariant in reference frames translating or rotating at constant velocity one from each other. Since the necessary condition (75) can be obtained in any of them, V_M should be understood as a velocity difference with respect to any uniform velocity (in an unbounded domain) or to any velocity field corresponding to solid body rotation. We may relate V_M and Λ_M by defining the scale $l \equiv V_M/\Lambda_M$. l is a characteristic scale related to velocity gradients. The problem is thus to determine whether H and l are independent or not. On one side, the magnetic field being generated by the velocity field, one may expect that H depends on l. On the other side, it is unlikely that H depends uniquely on l; it certainly depends on the flow geometry as can be seen by considering the form of the term responsible for possible dynamo action in (74) and (80). Then, it may be possible to vary H and l independently by tuning some

appropriate flow parameter. Thus, one have to locate the region where dynamo action is impossible in a two-parameter space, $(R_m, L/l)$ displayed in Fig. 7 where $R_m \equiv \mu_0 \sigma L V_M$.

The main difficulty is that the necessary conditions (75,81) involve the parameters H and Λ_M that are not directly controlled in an experiment. The above discussion illustrates that R_m is not the only relevant dimensionless parameter to describe dynamo onset. Indeed, the conditions (75,81) are not sufficient for dynamo action. We will discuss below examples of "antidynamo theorems" which show that dynamo action is impossible for particular geometries of the velocity and/or the magnetic fields.
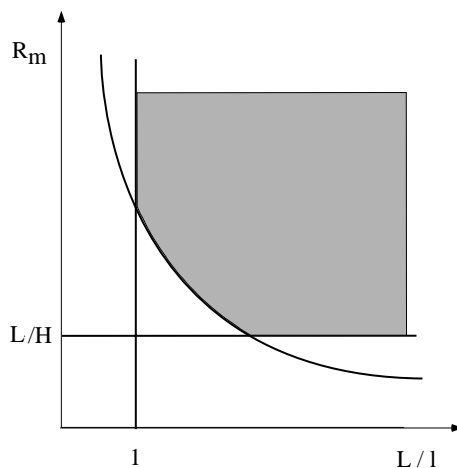

Figure 7. The necessary conditions (75,81) correspond to $R_m > L/H$ and $R_m > Ll/H^2$. Dynamo action is not possible outside the shaded region.

4.3. *"Antidynamo theorems"*

It has been first shown by Cowling in 1934 [26] that an axisymmetric magnetic field cannot be maintained by dynamo action. Several such "anti-dynamo theorems" have been found since. They state that either magnetic fields of given geometries cannot be generated by a fluid dynamo or that flows of given geometries cannot undergo a dynamo instability. Cowling's result belongs to the first class. It should be emphasized that it does not concern the problem of the dynamo capability of an axisymmetric flow. An axisymmetric flow may indeed generate a non axisymmetric magnetic field (see the section on laminar dynamos). On the contrary, it is known that,

two-dimensional flows i.e. with velocity fields with one vanishing component in cartesian coordinates [27], toroidal flows i.e. flows with a vanishing radial component in spherical geometry [28,25] do not lead to dynamo action. Most of these results have been extended to compressible flows and it has been also shown that a purely radial flow in spherical geometry cannot sustain a magnetic field [29]. Note however that a flow without radial component can generate a magnetic field in cylindrical geometry (see the section about laminar dynamos). It should be stressed that most of these results have not been demonstrated with all possible boundary conditions. Several demonstrations are also restricted to time independent magnetic fields which is clearly a too strong assumption. We will not give here the demonstrations of all the above results. For a review from a mathematical view point, we refer to Nunez [30].

5. Laminar dynamos

There exist very few laminar flows for which dynamo action can be shown analytically. This is partly due to "antidynamo theorems" that rule out many simple flows. Examples of analytically tractable dynamos are of great interest to understand the basic mechanisms that give rise to dynamo action. So one can get an idea about the flow properties responsible for its good dynamo capability. The kinematic dynamo problem is solved numerically in most cases. It should be noted that it is much more sensitive to truncation errors than most of the other hydrodynamic instabilities. Several examples of dynamos obtained in the past indeed resulted from a lack of numerical resolution or equivalently because a too small number of modes was kept. This extreme sensitivity with respect to resolution is certainly related to the geometry of the neutral magnetic modes which are often strongly localized in space.

We have already mentioned the rotor dynamo of Herzenberg [23] and its experimental demonstration by Lowes and Wilkinson [24]. Although these flows give rise to homogeneous dynamos, they may look somewhat artificial since the fact that they are not simply connected in space is an essential feature. A laminar flow in a simply connected domain displaying dynamo action was found by Lortz [31] but without any illustrative example. We will first consider in this section the Ponomarenko dynamo [32] which is driven by a very simple helical flow. This flow as well as other helical flows with more realistic velocity profiles are known to have the best dynamo capability among all the known laminar dynamos. We will next consider another class of flows for which the magnetic field is generated at a scale large compared to the one of the flow. This occurs for many spatially

periodic flows as shown by G. O. Roberts [33,34] and makes the analysis much simpler. Finally, we will make some comments related to the nature of the bifurcation corresponding to the dynamo onset (broken symmetries, Hopf or stationary bifurcation, etc).

5.1. The Ponomarenko dynamo

5.1.1. Linear stability analysis

The Ponomarenko dynamo consists of a cylinder of radius R, in solid body rotation at angular velocity ω, and translation along its axis at speed V, embedded in an infinite static medium of the same conductivity with which it is in perfect electrical contact (Figure 8). Using respectively, R, $\mu_0 \sigma R^2$, $(\mu_0 \sigma R)^{-1}$, as units for length, time and velocity, the governing equation for the magnetic field, $\vec{B}(\vec{r}, t)$, is

$$\frac{\partial \vec{B}}{\partial t} = \nabla \times (\vec{v} \times \vec{B}) + \nabla^2 \vec{B}. \tag{82}$$

The kinematic dynamo problem, i.e. the linear stability analysis of the solution $B = 0$ of (82), is governed by two dimensionless numbers

$$R_m = \mu_0 \sigma R \sqrt{(R\omega)^2 + V^2}, \quad Ro = \frac{V}{R\omega}. \tag{83}$$

The dimensionless velocity field is

$$\vec{v} = \begin{pmatrix} 0 \\ rR_m/\sqrt{1 + Ro^2} \\ R_m/\sqrt{1 + Ro^{-2}} \end{pmatrix} \quad \text{for } r < 1 \tag{84}$$

and vanishes for $r > 1$. The neutral modes are of the form

$$\vec{B}(\vec{r}, t) = \vec{b_p}(r) \exp i(\omega_0 t + m\theta + kz). \tag{85}$$

We have a Hopf bifurcation if $\omega_0 \neq 0$ and a stationary bifurcation otherwise.

We write equation (82) in the form

$$L\vec{B} \equiv \frac{\partial \vec{B}}{\partial t} - \nabla \times (\vec{v} \times \vec{B}) - \nabla^2 \vec{B} = 0, \tag{86}$$

and get for magnetic fields of the form (85)

$$L_r \vec{b_p} \equiv i(\omega_0 + \mu \Gamma(r))\vec{b_p} - \Delta \vec{b_p} + D_l \vec{b_p} = 0, \tag{87}$$

where $\mu = (\mu_0 \sigma R^2)(m\omega + kv)$ and $\Gamma(r) = 1$ for $r < 1$ and $\Gamma(r) = 0$ for $r > 1$.
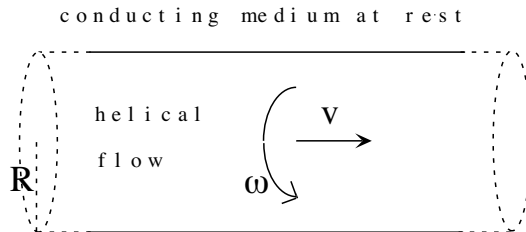
conducting medium at rest

helical flow

R

V

ω

Figure 8. Sketch of the Ponomarenko dynamo.

The operator Δ traces back to Joule dissipation in the induction equation,

$$\Delta = \begin{pmatrix} l. - \frac{1}{r^2} & -\frac{2im}{r^2} & 0 \\ \frac{2im}{r^2} & l. - \frac{1}{r^2} & 0 \\ 0 & 0 & l. \end{pmatrix} \,, \tag{88}$$

where l is an operator defined by

$$l.f = \frac{1}{r}\frac{d}{dr}\left(r\frac{df}{dr}\right) - (\frac{m^2}{r^2} + k^2)f \,. \tag{89}$$

Note that the non diagonal terms of Δ couple the radial and azimuthal components of the magnetic field. The coupling vanishes if $m = 0$ for which dynamo action is impossible in agreement with Cowling anti-dynamo theorem (the magnetic field being axisymmetric). We emphasize that this coupling, essential for dynamo action, results from Joule dissipation, and governs the large R_m behavior of the Ponomarenko dynamo. It could be understood as an "α-effect" (see below).

D_l results from the velocity discontinuity for $r = 1$. Its expression,

$$D_l = \begin{pmatrix} 0 & 0 & 0 \\ R\omega\delta(r-1) & 0 & 0 \\ V\delta(r-1) & 0 & 0 \end{pmatrix} \,, \tag{90}$$

shows how the shear at $r = 1$ generates the azimuthal and axial components of the field from the radial one. As explained in the section on advection and diffusion of a passive vector, the magnetic field tends to become aligned with the shear flow. This can be also understood as an "ω-effect". The discontinuity of the derivatives of the θ and z-components of the magnetic field at $r = 1$ is thus proportional to the value of B_r.

Thus, we can understand qualitatively the mechanism of Ponomarenko dynamo: a perturbation B_r gives rise to B_θ and B_z under the action of the

shearing motion along θ and z at $r = 1$. B_r is then regenerated by Joule diffusion of B_θ provided that $m \neq 0$. We note that this mechanism subsists for more realistic helical flows without a discontinuity for $r = 1$. Smoothing the discontinuity thus creating a region of width δ with strong shear in the vicinity of $r = 1$, does not affect qualitatively the above mechanism; only the limit $R_m \to \infty$ or any other limit involving spatial scales small compared to δ may be affected.

The dynamo threshold can be found by solving equation (87) for $r < 1$ and $r > 1$ and then writing boundary conditions at $r = 1$. We first note that we have only to find b_r et b_θ. Indeed, $\vec{B}$ being solenoidal,

$$\frac{1}{r}\frac{d(rb_r)}{dr} + \frac{im}{r}b_\theta + ikb_z = 0\,. \tag{91}$$

Defining $b_\pm = b_r \pm ib_\theta$, we get

$$\frac{1}{r}\frac{d}{dr}\left(r\frac{db_\pm}{dr}\right) - \left(\frac{(m \pm 1)^2}{r^2} + (k^2 + p + i\mu\Gamma(r))\right)b_\pm = 0. \tag{92}$$

$b_\pm$ are thus decoupled for $r < 1$ and $r > 1$ and the solutions are given by the Bessel functions $I(n,x)$ et $K(n,x)$ [21]. In order to avoid divergence of the solutions for $r = 0$ and $r \to \infty$, we take

$$r \leq 1 \quad b_\pm = A_\pm \frac{I(m\pm 1, qr)}{I(m\pm 1, q)} \text{ with } q^2 = p + k^2 + i\mu\,, \tag{93}$$

$$r \geq 1 \quad b_\pm = B_\pm \frac{K(m\pm 1, sr)}{K(m\pm 1, s)} \text{ with } s^2 = p + k^2\,. \tag{94}$$

The four unknowns, $A_\pm$ et $B_\pm$ are determined by boundary conditions at $r = 1$. The normal component of $\vec{B}$ and the tangential components of $\vec{H}$ and therefore of $\vec{B}$ being continuous, $b_\pm$ should be continuous and thus, $A_\pm = B_\pm$. The continuity of $\vec{B}$ and (91) imply that db_r/dr is continuous. Finally, the continuity of the tangential component of the electric field implies that $db_\theta/dr + v_\theta b_r$ is continuous. We thus have four unknowns and four conditions. The existence of non trivial solutions for $A_\pm$ requires

$$R^+ R^- = \frac{i\omega}{2}(R^+ - R^-)\,, \tag{95}$$

where

$$R^\pm = q\frac{I'(m \pm 1, q)}{I(m \pm 1, q)} - s\frac{K'(m \pm 1, s)}{K(m \pm 1, s)}\,. \tag{96}$$

The numerical resolution of this equation gives the growth rate $p = \Phi(R_m, Ro, k, m)$ where Φ is a function of the parameters R_m, Ro, k, m. At the instability onset, $Re(p) = 0$ gives the critical magnetic Reynolds number for dynamo action $R_{mc} = \Psi(Ro, k, m)$. The minimum corresponds to $m = 1$, $Ro = 1.314$, $k = k_c = -0.38$, for which we have $R_{mc} = 17.72$ and

$\omega_0 = 0.410$. We thus have a Hopf bifurcation. $m = 0$ is impossible from Cowling's anti-dynamo theorem and m larger than 1 leads to an increased Joule dissipation. We note that the maximum dynamo capability of the flow (R_{mc} minimum) is obtained when the azimuthal and axial velocities are of the same order of magnitude ($Ro \sim 1$). This trend is often observed with more complex flows for which the maximum dynamo capability is obtained when the poloidal and toroidal flow components are comparable. Finally, note that the pitches of the helices of the magnetic field and of the velocity field are opposite but not equal in magnitude such that $\mu \neq 0$. The magnetic field becomes more and more aligned with the shear at large R_m and the kinematic problem is easier to solve for modes with a wavelength small compared to R [3,35,36] . We show next that the dynamo onset occurs in a high R_m limit when $Ro \to 0$, which makes its study simpler.
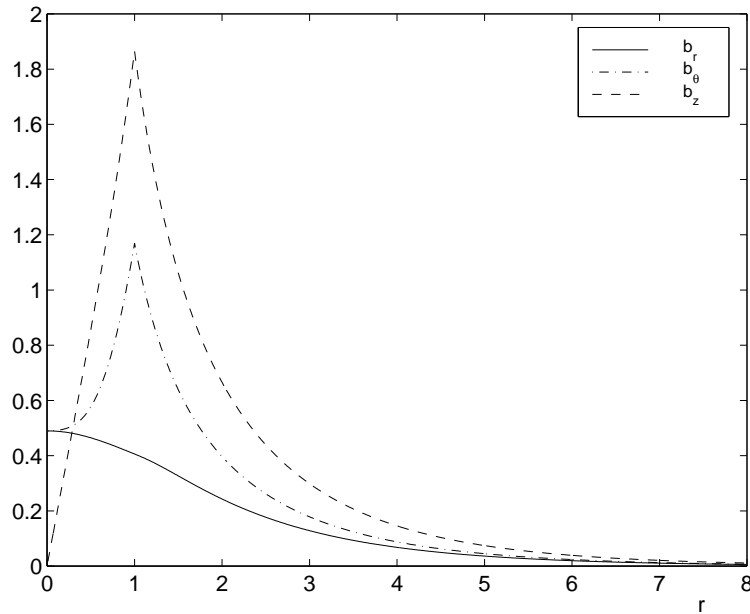

Figure 9.   Absolute value of the components of the unstable mode of the Ponomarenko dynamo.

5.1.2. *The high rotation rate limit*

Although R_{mc} tends to infinity, the linear stability analysis becomes simpler in the limit of high rotation rate, $Ro \to 0$. The field is mostly sheared in the azimuthal direction and thus $k_c \to \infty$. The argument of the Bessel functions then tends to infinity and it is possible to use their asymptotic expressions. We thus obtain

$$R_{mc} = 4\sqrt{2}Ro^{-3} , \tag{97}$$

$$\omega_o = \sqrt{3}Ro^{-2} , \tag{98}$$

$$k_c = -Ro^{-1} , \tag{99}$$

$$\mu \ll \omega_o . \tag{100}$$

R_{mc} tends to infinity because the flow becomes two dimensional in the limit $Ro \to 0$, for which dynamo action becomes impossible. Note however that the wavelength of the neutral mode vanishes proportionally to Ro. Thus, at the spatial scale of the neutral mode, the flow remains three-dimensional and dynamo action remains possible for any value of Ro. This last result may be modified if the velocity discontinuity is smoothed.

The validity of our asymptotic calculation is checked by comparing the above results to the ones obtained by numerically solving the full problem (Figure 10). The agreement is good even for $Ro \sim 1$.

The expressions for the fields are also simpler in the high rotation rate limit. Writing $q = \sqrt{2}e^{i\pi/6}Ro^{-1}$, we get for $r \le 1$

$$b_r = \frac{1}{2}\Big(\frac{I(2,qr)}{I(2,q)} - \frac{I(0,qr)}{I(0,q)}\Big) - \frac{1}{q^2}\frac{I(0,qr)}{I(0,q)} ,$$
$$b_\theta = \frac{1}{2i}\Big(\frac{I(2,qr)}{I(2,q)} + \frac{I(0,qr)}{I(0,q)}\Big) + \frac{1}{iq^2}\frac{I(0,qr)}{I(0,q)} , \tag{101}$$

and for $r \ge 1$

$$b_r = \frac{1}{2}\Big(\frac{K(2,qr)}{K(2,q)} - \frac{K(0,qr)}{K(0,q)}\Big) - \frac{1}{q^2}\frac{K(0,qr)}{K(0,q)} ,$$
$$b_\theta = \frac{1}{2i}\Big(\frac{K(2,qr)}{K(2,q)} + \frac{K(0,qr)}{K(0,q)}\Big) + \frac{1}{iq^2}\frac{K(0,qr)}{K(0,q)} , \tag{102}$$

from which b_z can be computed using $\vec{\nabla} \cdot \vec{B} = 0$. The field components are displayed in Figure 11. The field becomes more and more localized close to $r = 1$ when $Ro \to 0$. From the qualitative description of the mechanisms responsible for the Ponomarenko dynamo, B_θ (respectively B_z) is generated from B_r by the velocity shear $R\omega$ (respectively V). Thus, we expect $B_z \propto RoB_\theta$. B_r is regenerated from B_θ, thus $B_r \propto Ro^2 B_\theta$ (from equations (87, 88) and $\omega_0 \propto Ro^{-2}$).
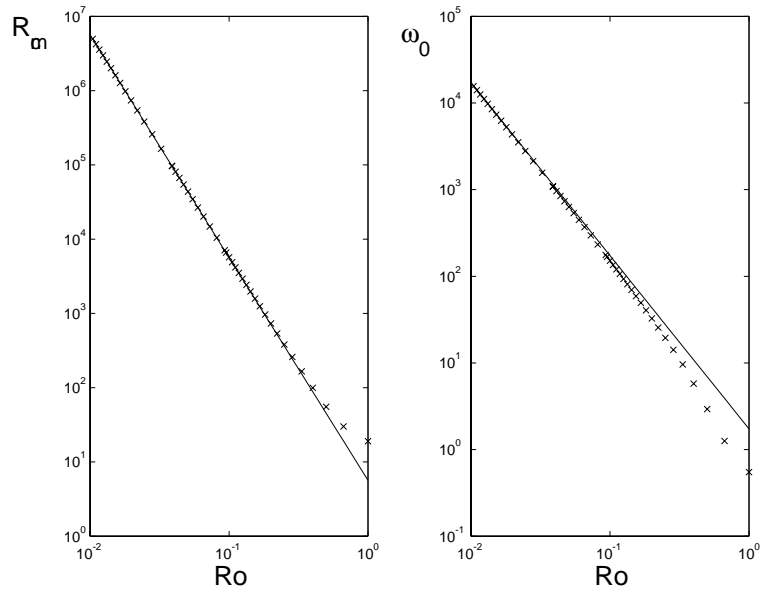
Figure 10.   Critical magnetic Reynolds number R_{mc} and pulsation at onset ω_0 as a function of the Rossby number Ro. The cross are numerical solutions of equation (95). The full line is the asymptotic solution given by equations (97) and (98).

5.1.3. *Further remarks on the Ponomarenko dynamo*

As already mentioned, the velocity discontinuity is a rather unrealistic feature of the Ponomarenko dynamo. If the solid rotor is replaced by the helical flow of a liquid metal, the velocity field then becomes of the form $\vec{v} = (0, v_\theta(r), v_z(r))$ and should vanish for $r = 1$. The corresponding kinematic dynamo problem has been studied theoretically [35,36] and self-generation of the magnetic field has been observed experimentally (Riga experiment) [37]. Although this decreases the value of R_{mc}, the presence of an external conducting medium is not required any more when the velocity profile depends on r. In the case of solid body rotation and translation, the presence of a conducting external medium is necessary because the dynamo problem is unchanged in reference frames rotating and translating at constant velocity one from each other; thus, the Ponomarenko problem is unchanged if the rotor is static and the external medium moves at velocity $-V$ along the z-axis with a rotation rate $-\omega$. With an insulating external medium, this motion obviously cannot drive any dynamo. The dynamo capability of helical flows remains almost unchanged with realistic velocity
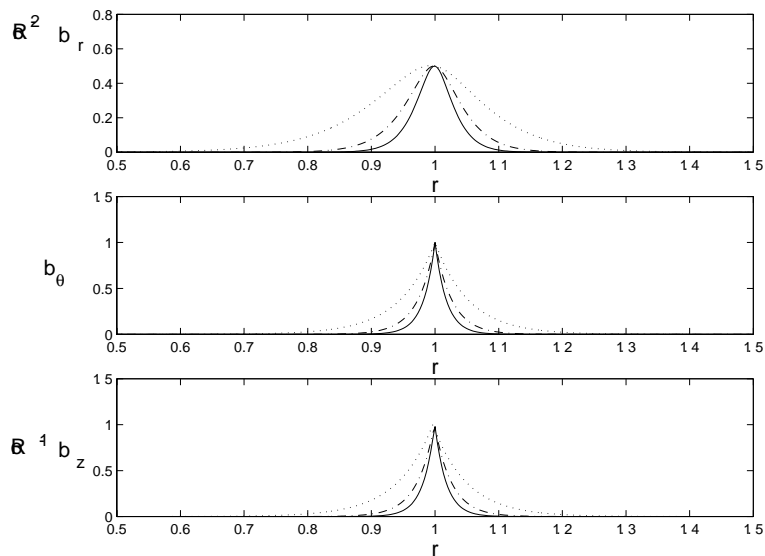
Figure 11.   Absolute value of the components of the unstable mode of the Ponomarenko dynamo in the small Rossby number limit: $Ro^{-1} = 15$ (dotted lines), $Ro^{-1} = 30$ (dash-dotted lines), $Ro^{-1} = 45$ (full lines).

profiles. Indeed, a critical magnetic Reynolds number of order 20 has been observed in the experiments [37]. On the contrary, the behavior of the growth rate for $R_m \to \infty$ strongly depends on the flow profile. With a smooth helical flow, the growth rate decreases to zero when $R_m \to \infty$ whereas it tends to a finite value in the case of the Ponomarenko dynamo [36]. With a smooth flow, the regeneration of B_r from B_θ vanishes in the limit $R_m \to \infty$ because it is due to Joule dissipation. This does not occur with the discontinuous profile because the most unstable wavenumber can increase with R_m thus keeping the effect of Joule dissipation constant in the limit $R_m \to \infty$.

5.2. *Spatially periodic dynamos*

It has been shown by G. O. Roberts [33,34] that many spatially periodic flows generate a magnetic field at a large scale compared to their spatial periodicity. After discussing the importance of this scale separation, we present two examples of such flows.

5.2.1. *Scale separation*

We have already mentioned that the term $(\vec{B} \cdot \vec{\nabla})\vec{v}$ is the main source term for the amplification of the magnetic field which is dissipated by the diffusive term $\nu_m \nabla^2 \vec{B}$. Thus, self-generation of a large scale magnetic field looks easier because Joule dissipation per unit volume vanishes if the wavelength of the field tends to infinity. This has obviously some cost since it requires to drive a flow in a very large domain. If the magnetic field is generated on spatial scale L, large compared to the one of the velocity field, l, we may define the magnetic Reynolds number as usual with the ratio of the above two terms and get: $R_{m1} = \mu_0 \sigma V L^2 / l = P_m Re(L/l)^2$, where $P_m = \mu_0 \sigma \nu$ is the magnetic Prandtl number and $Re = Vl/\nu$ is the Reynolds number of the flow. This definition is strongly misleading because it gives the impression that increasing scale separation, i.e. increasing L/l, may be as efficient as increasing $\mu_0 \sigma$ or the flow velocity to get dynamo action. This is of course not true in general. There are three independent dimensionless parameters in the problem, R_{m1}, Re, L/l or alternatively, R_{m1}, P_m, L/l. The critical magnetic Reynolds number is thus of the form

$$R_{m1}^c = f(P_m, L/l) \,, \tag{103}$$

where f is an arbitrary function at this stage. The dependence on P_m means that the dynamo capability of the flow may depend on its level of turbulence (see next section). The dependence on L/l determines whether scale separation is good for dynamo action. This of course depends on the criterion we choose: let us first take a minimum kinetic Reynolds number for a given fluid. Assuming a dependence of the form $(L/l)^n$, one should have $n < 2$ in order to take profit from scale separation. It is likely that $n > 0$ because the large scale magnetic field cannot be generated without a small scale component driven by the interaction of the small scale flow with the large scale magnetic field. The resulting small scale magnetic field leads to an increased dissipation and thus to a larger value of R_{m1}^c. It is even likely that $n > 1$, otherwise it will be possible to generate a dynamo for fixed L just by taking the limit $l \to 0$, some sort of "microdynamo" !

We consider a spatially periodic velocity field with wavelength l and assume that a magnetic field $\vec{B}_0$ is generated on a spatial scale L. As said above, a field with spatial periodicity l is generated by the interaction of $\vec{B}_0$ with the flow. We thus write

$$\vec{B} = \vec{B}_0 + \vec{b} \,, \tag{104}$$

with $\langle \vec{b} \rangle = 0$ where $\langle \cdot \rangle$ stands for the spatial average on one wavelength l. Inserting (104) in the induction equation, and averaging over space, we get

the evolution equation for the mean field $\vec{B}_0$

$$\frac{\partial \vec{B}_0}{\partial t} = \vec{\nabla} \times \langle \vec{v} \times \vec{b} \rangle + \nu_m \Delta \vec{B}_0. \tag{105}$$

Subtracting (105) from the induction equation, we get the evolution equation for the fluctuating field $\vec{b}$

$$\frac{\partial \vec{b}}{\partial t} = \vec{\nabla} \times \left(\vec{v} \times \vec{B}_0 + \vec{v} \times \vec{b} - \langle \vec{v} \times \vec{b} \rangle \right) + \nu_m \Delta \vec{b}. \tag{106}$$

We have to find $\vec{b}$ as a function of $\vec{B}_0$ using equation (106) in order to get a closed equation for the mean field from (105). (106) may be solved easily if $\vec{b}$ is small compared to $\vec{B}_0$; we then have at leading order a diffusion equation for $\vec{b}$ with a source term depending on $\vec{B}_0$ and the velocity field. Then, we get

$$\nu_m \frac{b}{l^2} \sim \frac{v B_0}{l}, \quad \text{thus} \quad b \sim \frac{vl}{\nu_m} B_0. \tag{107}$$

Using this expression of b in order to estimate $\langle \vec{v} \times \vec{b} \rangle$ which does not depend any more on l after being averaged, we get from (105) the following condition for dynamo onset

$$\frac{v_c^2 l}{\nu_m} \frac{B_0}{L} \sim \frac{\nu_m B_0}{L^2}, \quad \text{thus} \quad v_c \sim \frac{\nu_m}{\sqrt{Ll}}. \tag{108}$$

We first observe that $b \sim \frac{\sqrt{lL}}{B}_0 \ll B_0$ provided that $l \ll L$. We have for the Reynolds number of the flow $Re \sim \sqrt{\frac{l}{L}} P_m^{-1} \ll 1$ if P_m is not too small. The magnetic Reynolds number at dynamo onset is $R_{m1}^c = \mu_0 \sigma v_c L^2 / l \sim (L/l)^{3/2} \gg 1$, thus $n = 3/2$. We observe that the relevant definition here for the magnetic Reynolds number would be

$$R_{m2} \equiv \mu_0 \sigma v \sqrt{Ll}, \tag{109}$$

the critical value of which for dynamo onset is $R_{m2} \sim 1$. Consequently, even if the above mechanism works, we cannot reach the dynamo onset just by increasing scale separation. For ν_m and v fixed, it does not help to decrease l. Whether scale separation makes easier the experimental observation of the dynamo effect still deserves more discussion (see next section). At this stage, scale separation makes possible to keep the kinetic Reynolds number small at dynamo onset. However, with a realistic value of P_m ($P_m \sim 10^{-5}$), one needs an enormous scale separation. With P_m of order 1, the critical magnetic Reynolds number is small if it is defined with l only but is of order $\sqrt{L/l} \gg 1$ if it is defined with L only. The main advantage of scale separation is that it makes analytical calculations much

easier. This is a general feature of long wavelength instabilities associated with hydrodynamic modes, i.e. modes with vanishing growth rate at zero wavenumber [38]. We will illustrate this below.

5.2.2. *The G. O. Roberts' dynamo*

We consider the spatially periodic flow of velocity field

$$\vec{v}(x,y,z) = \begin{pmatrix} U \sin ky \\ U \cos kx \\ V(\sin kx + \cos ky) \end{pmatrix} . \tag{110}$$

We have $\langle \vec{v} \rangle = 0$ and the mean helicity is $h = \langle \vec{v} \cdot \vec{\nabla} \times \vec{v} \rangle = -2kUV$. Assuming that b is small compared to B_0, we get from equation (106)

$$\vec{b} \approx \frac{1}{\nu_m k} \begin{pmatrix} U B_2 \cos ky \\ -U B_1 \sin kx \\ V B_1 \cos kx - V B_2 \sin ky \end{pmatrix} , \tag{111}$$

where $\vec{B}_0 = (B_1, B_2, B_3)$. We thus get

$$\langle \vec{v} \times \vec{b} \rangle \approx \frac{UV}{\nu_m k} \begin{pmatrix} 1 & 0 & 0 \\ 0 & 1 & 0 \\ 0 & 0 & 0 \end{pmatrix} \vec{B}_0 . \tag{112}$$

We observe that if a large scale field exists along the x or y-axis, the co-operative effect of small scale periodic fluctuations is to drive a current parallel to the large scale field. This has been understood by Parker [39] and is due to the helical nature of the flow. Any field B_1 along the x-axis is distorted in the vertical plane $x - z$ by the z-component of the flow of amplitude V. The field is twisted out of the $x - z$ plane by the toroidal component of the flow of amplitude U. This drives field loops in the $y - z$ plane, i.e. a current parallel to x, which generates a magnetic field with a non-zero component along the y-axis, B_2. B_2 can then regenerate B_1 through the same process. The mean electromotive force $\langle \vec{v} \times \vec{b} \rangle$ in the mean field equation (105) was described by Steenbeck and Krause in 1966 as the "α-effect" (see for instance [8]). In this terminology, G. O. Roberts' dynamo is an α^2-dynamo. Defining $\alpha = UV/\nu_m k$, we have for a mean field of the form $\vec{B}_0(Z,T) = (B_1, B_2, 0)$,

$$\frac{\partial B_1}{\partial T} = -\alpha \frac{\partial B_2}{\partial Z} + \nu_m \frac{\partial^2 B_1}{\partial Z^2} , \tag{113}$$

$$\frac{\partial B_2}{\partial T} = \alpha \frac{\partial B_1}{\partial Z} + \nu_m \frac{\partial^2 B_2}{\partial Z^2} , \tag{114}$$

Defining $A = B_1 + iB_2$, we get

$$\frac{\partial A}{\partial T} = -i\alpha \frac{\partial A}{\partial Z} + \nu_m \frac{\partial^2 A}{\partial Z^2} \,, \qquad (115)$$

The linear stability analysis of the solution $A = 0$ (i.e. $\vec{B} = 0$) is straightforward. We consider normal modes of the form $A \propto \exp(\eta T \pm iKZ)$ and get from (115) the dispersion relation

$$\eta = \pm|\alpha K| - \nu_m K^2, \qquad (116)$$

which shows that there exists a branch of unstable modes at long enough wavelength ($K < |\alpha|/\nu_m$).

We observe that dynamo action vanishes if $U \to 0$ or $V \to 0$ in agreement with antidynamo theorems. It is interesting to consider the behavior of α when the magnetic Reynolds number becomes larger. To wit, the calculation of $\vec{b}$ should be performed at higher orders in equation (106). Solving perturbatively this equation for $\vec{b}$ as an expansion in powers of $U/\nu_m k$, one gets

$$\alpha = \frac{UV}{\nu_m\, k} \left(1 - \frac{U^2}{2\, \nu_m{}^2\, k^2} + ... \right) \,. \qquad (117)$$

α increases linearly with V but its behavior as a function of U is more complex. It first increases but reaches a maximum and then decreases as U is increased. This behavior is due to the expulsion of the transverse field by the rotating eddies as already shown in [40] by numerically solving (106). It has been found that α decreases toward zero at large R_m. Note however that the large R_m limit should be considered carefully. As said above, the great simplification of scale separation results from the fact that the magnetic Reynolds number evaluated on the small scale of the flow is small whereas the one evaluated on the large scale of the mean field is large. This is clearly apparent in our second order result (117). Truncating the expansion in $U/\nu_m\, k$ is not accurate if R_m is too large such that the magnetic Reynolds number related to the azimuthal motion of the eddies becomes of order 1.

The α-effect has been demonstrated experimentally by directly measuring the mean electromotive force generated by an helical flow of liquid sodium submitted to an external magnetic field [41]. Self-generation of a magnetic field by the α-effect has been achieved recently, using a periodic arrangement of counter-rotating and counter-current helical vortices that mimic G. O. Roberts' flow. Axial and azimuthal sodium flows are driven by pumps in an array of helical ducts immersed in a cylinder (Karlsruhe experiment) [42].

5.2.3. *The ABC dynamo*

The mean electromotive force $\langle \vec{v} \times \vec{b} \rangle$ can be proportional to $\vec{B}_0$ when the flow is more symmetric than the one considered above. This can be achieved with the "ABC" flow

$$\vec{v}(x, y, z) = V \begin{pmatrix} \sin ky + \cos kz \\ \sin kz + \cos kx \\ \sin kx + \cos ky \end{pmatrix} . \tag{118}$$

We have $\langle \vec{v} \rangle = 0$ and the mean helicity is $h = \langle \vec{v} \cdot \vec{\nabla} \times \vec{v} \rangle = -3kV^2$. Using the same procedure as above, we get

$$\langle \vec{v} \times \vec{b} \rangle \approx \frac{2V^2}{\nu_m k} \vec{B}_0 . \tag{119}$$

Thus, the mean field $\vec{B}_0$ is governed by the equation

$$\frac{\partial \vec{B}_0}{\partial T} = \alpha \vec{\nabla} \times \vec{B}_0 + \nu_m \Delta \vec{B}_0. \tag{120}$$

We consider normal modes of the form $\vec{B}_0 = \hat{B}_0 \exp(\eta T \pm i \vec{K} \cdot \vec{R})$ and get from (120) the dispersion relation (116).

A mean field equation of the form (120) is expected to leading order for any small scale flow which is spatially homogeneous and isotropic. Indeed, for a given velocity field, we expect from equation (106) that $\vec{b}$ is linearly related to $\vec{B}_0$, thus the mean electromotive force $\langle \vec{v} \times \vec{b} \rangle$ is linearly related to $\vec{B}_0$. If we assume that, due to scale separation, there exists an expansion of $\langle \vec{v} \times \vec{b} \rangle$ as a function of $\vec{B}_0$ and its gradients, we get

$$\langle \vec{v} \times \vec{b} \rangle_i = \alpha_{i,j} B_0 {}_j + \beta_{i,j,k} \frac{\partial B_0 {}_j}{\partial x_k} + \cdots , \tag{121}$$

where the components of the tensors $\alpha_{i,j}$ and $\beta_{i,j,k}$ are functionals of the velocity field, i.e. depend on its moments. If the flow is isotropic, $\alpha_{i,j}$ and $\beta_{i,j,k}$ should be isotropic tensors, thus $\alpha_{i,j} = \alpha \, \delta_{i,j}$ and $\beta_{i,j,k} = \beta \, \epsilon_{i,j,k}$. Consequently,

$$\langle \vec{v} \times \vec{b} \rangle = \alpha \vec{B}_0 - \beta \vec{\nabla} \times \vec{B}_0 + \cdots , \tag{122}$$

and

$$\frac{\partial \vec{B}_0}{\partial T} = \alpha \vec{\nabla} \times \vec{B}_0 + \nu_t \Delta \vec{B}_0 , \tag{123}$$

where $\nu_t = \nu_m + \beta$ is the "turbulent" magnetic diffusivity. As said above, the α-effect is always dominant at large enough scale and leads to dynamo action provided that $\alpha \neq 0$. For helical flows, α is proportional to the mean helicity but it has been shown that a non-zero mean helicity is not necessary

for the α-effect [45]. However, the flow should not be parity invariant; indeed, if the flow is symmetric with respect to some plane, $\alpha[S.\vec{v}] = \alpha[\vec{v}]$ where S is the corresponding symmetry transformation. On the other side, $\vec{B}_0$ being a pseudo-vector, it does not transform in the same way as $\vec{\nabla} \times \vec{B}_0$ under S. Consequently (123) implies $\alpha = 0$ and one has to consider the effect of higher order terms. We have often $\beta > 0$, i.e. the magnetic diffusivity is usually enhanced by the small scale flow but periodic flow configurations with $\beta < 0$ have been also reported [43].

5.2.4. *Further remarks on the dynamo bifurcation*

- Hopf versus stationary bifurcations

We have studied previously two examples of laminar dynamos generated by stationary flows: Ponomarenko's and the G. O. Roberts' dynamos. The first one is generated through a Hopf bifurcation, the second is stationary. Why ? Although general predictions about the nature of the bifurcation cannot be made, some features can be understood using symmetry considerations [46]. Ponomarenko's flow is invariant under translations along the z axis $z \to z + z_0$. However, it is not invariant under $z \to -z$ (the helicity is changed to its opposite). In other words, the $+z$ and $-z$ directions are not equivalent. When the neutral mode breaks the translation invariance along z at bifurcation threshold, it naturally begins to drift in a direction depending on the sign of the helicity, thus $\omega_0 \neq 0$ and we have a Hopf bifurcation.

G. O. Roberts' flow also has a non-zero mean helicity. Moreover, it looks like a periodic array of helical flows with axis parallel to z. Why does it undergo a stationary bifurcation ? This is due to an additional symmetry: a rotation of angle π along the axis $x = y$ leaves the flow unchanged but would change the direction of propagation for a oscillatory instability. In general, we cannot rule out a Hopf bifurcation but we understand why it is not compulsory any more.

- The definition of R_m may be misleading

The definition of the magnetic Reynolds number, $R_m = \mu_0 \sigma V L$ usually involves the typical velocity V and the characteristic spatial scale L of the flow. In the case of scale separation, we have observed that we may replace L by $\sqrt{Ll}$ where l is the flow periodicity and L the typical size of the flow volume. All magnetic modes decay if R_m is small enough. Is it enough to increase R_m up to a high enough value to get one growing mode ? Even for flows that do generate a dynamo, the answer is no. This may be illustrated by the G. O. Roberts' example: we observed that the efficiency of the α-

effect decreases because of magnetic field expulsion if the toroidal flow U becomes too large (117). Thus, if V is too small, we cannot expect to generate a dynamo by increasing U. Moreover, there are many ways to increase U and V simultaneously ($U \propto V^n$ for instance) for which we may not generate a dynamo either. The growth rate of some magnetic modes will increase starting from a negative value, but decrease again as soon as expulsion becomes important and possibly before reaching dynamo action. Several numerical simulations display such a behavior [13,47,48]. We think that this is primarily due to the definition of R_m using the spatial scale of the flow instead of the one of the magnetic field neutral mode, i.e. L instead of H defined by (73). The magnetic neutral modes may become more and more localized at large R_m, thus leading to an increased Joule dissipation. With expulsion in mind, one may take the typical scale of the skin effect, i.e. proportional to $R_m^{-1/2}$. Then, note that an increased Joule dissipation is not enough to explain the above behavior. One should assume that the processes leading to dynamo action, such as the α-effect in G. O. Roberts' dynamo, may become weaker when R_m is large.

- What are the relevant parameters to describe the dynamo bifurcation?

The typical scale of the neutral magnetic field is not known a priori, thus defining $R_m = \mu_0 \sigma H V$ is not very useful. Are there parameters that characterize the dynamo capability of a given flow? The three simple examples we already mentioned, due to Herzenberg, Ponomarenko and G. O. Roberts, all involve non-zero helicity. This obviously helps but is not necessary [45]. Both poloidal and toroidal flow components should be specified to characterize the dynamo capability of G. O. Roberts' flow and this is also true to less extent for Ponomarenko's flow, but obviously not important in Herzenberg's dynamo or in any dynamo generated by a flow without toroidal component. Consequently, some trends exist but we do not have any a priori characterization of the dynamo efficiency of a laminar flow.

6. Turbulent dynamos

6.1. *Dynamos generated by small scale turbulence ?*

The observation of large scale magnetic fields of astrophysical objects motivated the study of dynamos generated by turbulent motion at smaller spatial scale and faster time scale. Parker showed qualitatively how the cooperative effect of "cyclonic eddies" i.e. localized helical flows, occurring randomly in space and time, may generate a large scale magnetic field [39]. This mechanism was understood on a more quantitative basis by Steenbeck, Krause and Rädler and gave rise to the subject of "Mean-field magnetohy-

drodynamics" (see for instance [8,7]). We refer to these books for a detailed presentation of this topic and we will just give some comments here. The method is based on scale separation, just as shown for spatially periodic flows in the previous section. It should be noted however, that it has been first introduced in the context of turbulent flows. In the case of homogeneous isotropic flows lacking parity invariance, a mean electromotive force of the form (122) is expected from symmetry considerations. It leads to the mean field equation (123) and thus to an α-dynamo. More complex forms of electromotive forces have been also found for anisotropic turbulent flows or non homogeneous ones [8].

In the case of parity invariant flows, the α-effect vanishes but it has been shown that dynamo can result from negative turbulent diffusivity [43,44]. The effect of helicity on the dynamo threshold and on the statistical properties of the bifurcated regime has been studied using EDQNM closures [49]. In the case of non helical flows, it has been shown that the critical magnetic Reynolds number tends to a constant in the limit of high kinetic Reynolds number and is independent of the flow volume in the limit of large scale separation.

It is a very interesting prediction that a magnetic field with a large scale coherent part can be generated by transferring energy from a turbulent flow with a much shorter coherence length. However, it should be pointed that no laboratory observation of this effect has been performed so far and that the theoretical approach is rather phenomenological. From a mathematical point of view, it would be interesting to have a theory for bifurcations from a random state, as the ones we have for bifurcations of stationary or periodic solutions.

Finally, a turbulent flow without geometrical constraints usually involves a large range of spatial scales with the largest part of its kinetic energy at large scales. Moreover, from the discussion of the previous section, the appropriate magnetic Reynolds number for an α-dynamo is $R_{m2} = \mu_0 \sigma v \sqrt{Ll}$. If a large range of scales l exists, it appears that the largest one would be the most efficient one for dynamo action. Thus, the reasons that are invoked to justify scale separation in turbulent flows without geometrical constraints are not always very convincing. We will therefore discuss next the more realistic situation in which a turbulent flow involves a non-zero mean flow.

6.2. *The dynamo threshold at large kinetic Reynolds number*

With a characteristic velocity V of the solid boundaries driving the fluid motion, and a characteristic integral scale L of the flow, we can define two independent dimensionless numbers, the magnetic Reynolds number, $R_m = \mu_0 \sigma L V$, and the magnetic Prandtl number, $P_m = \mu_0 \sigma \nu$. We have thus, $R_m = Re P_m$, where Re is the kinetic Reynolds number of the flow. For most known fluid dynamos, the dynamo threshold R_{mc} is roughly in the range 10-100. For liquid metals, $P_m < 10^{-5}$, thus the kinetic Reynolds number at dynamo onset is larger than 10^6 and, consequently, the flow is strongly turbulent. This is unpleasant for the experimentalist. Indeed, the power needed to drive a turbulent flow scales like $P \propto \rho L^2 V^3$ and we have

$$R_m \propto \mu_0 \sigma \left(\frac{PL}{\rho} \right)^{1/3} . \qquad (124)$$

This formula has simple consequences: first, taking liquid sodium (the liquid metal with the highest electric conductivity), $\mu_0 \sigma \approx 10 \ m^{-2}s$, $\rho \approx 10^3 \, kg \, m^{-3}$, and with a typical lengthscale $L \approx 1$m, we get $P \approx R_m^3$; thus a mechanical power larger than 100 kW is needed to reach a dynamo threshold of the order of 50. Second, it is unlikely to be able to operate experimental dynamos at R_m large compared with R_{mc}. Indeed, it costs almost 10 times more power to reach $2R_{mc}$ from the dynamo threshold. In conclusion, most experimental dynamos should have the following characteristics:

- (i) they bifurcate from a strongly turbulent flow regime,
- (ii) they operate in the vicinity of their bifurcation threshold.

The Karlsruhe [42] and Riga [37] experiments share the above characteristics. Both flows are strongly spatially constrained to mimic G. O. Roberts, respectively Ponomarenko dynamos, but small scale turbulence cannot be avoided. Although it was not surprising that these flows generate dynamos, they provided several interesting results. Concerning their dynamo thresholds, a surprisingly good agreement has been observed with the ones computed assuming the flow laminar with velocity field $\langle \vec{V}(\vec{r}) \rangle$ where $\langle \cdot \rangle$ stands for the average in time. Thus, turbulent fluctuations have a small effect on the dynamo thresholds of Karlsruhe and Riga experiments. This may be related to their geometrical constraints and one may expect a much larger difference when the instantaneous velocity field strongly differs from the time averaged one even at large scales. We consider next the case of small turbulent fluctuations and look at their effect on the dynamo threshold of the mean flow using perturbation analysis.

6.3. *Effect of turbulence on the dynamo threshold*

Writing $\vec{V}(\vec{r}, t) = \langle \vec{V}(\vec{r}) \rangle + \vec{v}(\vec{r}, t)$, the problem is to study the effect of the fluctuating velocity field $\vec{v}(\vec{r}, t)$ on the dynamo mechanisms. We get from the induction equation (45)

$$\frac{\partial \vec{B}}{\partial t} = \vec{\nabla} \times (\langle \vec{V} \rangle \times \vec{B}) + \vec{\nabla} \times (\vec{v} \times \vec{B}) + \nu_m \Delta \vec{B}. \qquad (125)$$

For small fluctuations $\vec{v}(\vec{r}, t)$, turbulence may just act as a random multiplicative forcing, thus shifting the laminar dynamo threshold and modifying the dynamics of the self-generated field in the vicinity of threshold. As in other experimentally studied instability problems, multiplicative random forcing may generate intermittent bursting in the vicinity of instability onset [50,51]. This type of behavior, understood in the framework of blowout bifurcations in dynamical system theory [52], has been observed in a numerical simulation of the MHD equations [53]. In these simulations, P_m is of order one, and the flow is chaotic at the dynamo threshold but not fully turbulent.

In the limit of small fluctuations, one can calculate the threshold shift using a perturbation expansion. We write equation (125) using L, L^2/ν_m and V as units of length, time and velocity. We get

$$\frac{\partial B}{\partial t} = R_m \vec{\nabla} \times \left(\langle \vec{V} \rangle \times \vec{B} \right) + \delta \vec{\nabla} \times \left(\vec{v} \times \vec{B} \right) + \nabla^2 \vec{B}. \qquad (126)$$

To relieve notation we have kept the same names for the non dimensional fields. $R_m = V L / \nu_m$ is the magnetic Reynolds number related to the mean flow. δ is a small parameter that measures the turbulent perturbation amplitude. We then expand $\vec{B}$ and R_m in power of δ

$$\vec{B} = \vec{B}^{(0)} + \delta \vec{B}^{(1)} + \delta^2 \vec{B}^{(2)} + \dots,$$
$$R_m = R_m^{(0)} + \delta R_m^{(1)} + \delta^2 R_m^{(2)} + \dots, \qquad (127)$$

and write equation (126) at order zero in δ

$$L \vec{B}^{(0)} = \frac{\partial \vec{B}^{(0)}}{\partial t} - R_m^{(0)} \vec{\nabla} \times \left(\langle \vec{V} \rangle \times \vec{B}^{(0)} \right) - \nabla^2 \vec{B}^{(0)} = 0. \qquad (128)$$

This is the laminar dynamo problem. By hypothesis, the instability onset is the one without turbulent perturbation, $R_{mc}^{(0)}$. At next order in δ we get

$$L \vec{B}^{(1)} = R_m^{(1)} \vec{\nabla} \times \left(\langle \vec{V} \rangle \times \vec{B}^{(0)} \right) + \vec{\nabla} \times \left(\vec{v} \times \vec{B}^{(0)} \right). \qquad (129)$$

The solvability condition gives the first correction in threshold

$$R_m^{(1)} = -\frac{\left\langle \vec{C} | \vec{\nabla} \times \left(\vec{v} \times \vec{B}^{(0)} \right) \right\rangle}{\left\langle \vec{C} | \vec{\nabla} \times \left(\langle \vec{V} \rangle \times \vec{B}^{(0)} \right) \right\rangle} , \qquad (130)$$

where $\vec{C}$ is in the kernel of $L^{\dagger}$, the adjoint of L. We use a scalar product in which the average over the realizations of the perturbation is made. In that case, the average over the realizations of $\left\langle \vec{C} | \vec{\nabla} \times \left(\vec{v} \times \vec{B}^{(0)} \right) \right\rangle$ is proportional to the average of $\vec{v}$, the value of which is zero by hypothesis. Thus, the dynamo threshold is unchanged up to first order in δ, $R_m^{(1)} = 0$.

To calculate the next order correction, we write equation (126) at order two in δ and get

$$L \, \vec{B}^{(2)} = R_m^{(2)} \, \vec{\nabla} \times \left(\langle \vec{V} \rangle \times \vec{B}^{(0)} \right) + \vec{\nabla} \times \left(\vec{v} \times \vec{B}^{(1)} \right) . \qquad (131)$$

We then get the second order correction

$$R_m^{(2)} = -\frac{\left\langle \vec{C} | \vec{\nabla} \times \left(\vec{v} \times \vec{B}^{(1)} \right) \right\rangle}{\left\langle \vec{C} | \vec{\nabla} \times \left(\langle \vec{V} \rangle \times \vec{B}^{(0)} \right) \right\rangle} , \qquad (132)$$

where $\vec{B}^{(1)}$ is solution of

$$L\vec{B}^{(1)} = \vec{\nabla} \times \left(\vec{v} \times \vec{B}^{(0)} \right) . \qquad (133)$$

Here, there is no simple reason for the correction to be zero. Its computation requires the resolution of equation (133). In some simple cases, an analytical expression for $R_m^{(2)}$ can be calculated.

We have thus obtained that when the amplitude δ of turbulent fluctuations is small, the modification of the dynamo threshold is at least quadratic in δ. Consequently, we may understand why the thresholds measured in the Karlsruhe and Riga experiments are very close to the predictions using the mean flow $\langle \vec{V} \rangle$ and thus ignoring turbulent fluctuations (the order of magnitude of the level of turbulent fluctuations related to the mean flow is certainly less than 10% in these experiments).

As said above, in experiments with unconstrained flows, one expects fully developed turbulent fluctuations at all scales. It is then probable that the observed dynamo would strongly differ from the one computed as if it were generated by $\langle \vec{V}(\vec{r}) \rangle$ alone. Indeed, as mentioned above, there exist even simple phenomenological models of dynamos generated only by turbulent fluctuations with $\langle \vec{V}(\vec{r}) \rangle = 0$. The role of turbulent fluctuations at such large Reynolds numbers may be twofold: on one hand, they decrease the effective electrical conductivity and thus inhibit the dynamo action generated

by $\langle \vec{V}(\vec{r}) \rangle$ by increasing Joule dissipation [54]. On the other hand, they may generate a large scale magnetic field through the "α-effect" [8,7] or higher order similar effects [43,44] even if $\langle \vec{V}(\vec{r}) \rangle = 0$. Consequently, there may also exist a parameter range in which the threshold of the dynamo generated by the mean flow alone is decreased by turbulent fluctuations. The problem can thus be stated as follows: for a given driving of the flow, what is the dependence of the critical magnetic Reynolds number for dynamo onset, R_m^c, as a function of the magnetic Prandtl number or equivalently as a function of the kinetic Reynolds number of the flow. In particular, is it possible to predict the behavior of R_m^c in the limit of infinite kinetic Reynolds number, at least for some class of mean flow configurations. Experiments are the only way to give a clear cut answer to this question because direct numerical simulations cannot be performed at such high Reynolds number. On the other side, self-generation of magnetic field from turbulent velocity fluctuations when the measured mean flow alone is not a dynamo, is still a great experimental challenge.

6.4. *Is it useful to have scale separation?*

We have mentioned above that for a given fluid, dynamo action can be achieved with a smaller kinetic Reynolds number with scale separation if an α-effect operates. From an experimental viewpoint, a more appropriate criterion may be a minimum power consumption. Thus, the advantage of scale separation can be checked in the following way. Suppose that the total available power P is fixed but that it can be shared among N motors. The more efficient way to drive the flow, even if technically complicated, consists in an homogeneous repartition of the motors in the whole flow volume L^3. The distance l between two motors then verifies $N l^3 = L^3$. Assuming that the power is dissipated by turbulence, we get $P = N \rho v^3 l^2$, where v is the velocity of the flow. In the case of an α-dynamo, the onset occurs at a fixed value of $v \sqrt{l L}$. The power at onset is thus

$$ P \propto \frac{N^{5/6}}{L} \, . \tag{134} $$

One recovers the fact that increasing the size of the experiment leads to a lower P at onset. The dependence on N is surprising. For a fixed flow volume, an increase in the number of motors (equivalently, an increase in scale separation) leads to a higher onset! This means that increasing scale separation is not usefull when the total power of the motors and the volume of the experiment are fixed.

7. Saturation of the magnetic field above the dynamo threshold

In this last section, we take into account the back reaction of the magnetic field generated above the dynamo threshold on the velocity field. We thus try to solve the dynamic dynamo problem, or in other words, to find a nonlinear equation for the amplitude of the linearly unstable mode at the bifurcation. Solving this equation determines the sub-critical or supercritical nature of the bifurcation and in the later case, the amplitude of the magnetic field as a function of the distance to the dynamo threshold. We recall the induction (45) and Navier-Stokes (21) equations that we restrict to incompressible flows ($\vec{\nabla} \cdot \vec{v} = 0$),

$$\frac{\partial \vec{B}}{\partial t} = \vec{\nabla} \times \left(\vec{v} \times \vec{B} \right) + \frac{1}{\mu_0 \sigma} \Delta \vec{B}, \tag{135}$$

$$\frac{\partial \vec{v}}{\partial t} + (\vec{v}.\vec{\nabla})\vec{v} = -\vec{\nabla} \left(\frac{p}{\rho} + \frac{B^2}{2\mu_0} \right) + \nu \Delta \vec{v} + \frac{1}{\mu_0 \rho}(\vec{B} \cdot \vec{\nabla})\vec{B}. \tag{136}$$

The flow is created, either by moving solid boundaries or by a body force added to the Navier-Stokes equation. We have to develop equations (135, 136) close to the dynamo threshold in order to derive an amplitude equation for the growing magnetic field. In general, this calculation is tractable only in the unrealistic case $P_m \gg 1$ such that the dynamo bifurcates from a laminar flow. For $P_m \ll 1$, a lot of hydrodynamic bifurcations occur first and the flow becomes turbulent before the dynamo threshold. We first present the structure of this perturbation analysis and solve explicitly a simple case that consists of a Ponomarenko type flow [55]. We then discuss the realistic situation ($P_m \ll 1$) and, using dimensional or phenomenological arguments, show that the expression of the generated magnetic field as a function of the fluid parameters strongly differs from the case $P_m \gg 1$.

7.1. *Laminar dynamos*

7.1.1. *Structure of the perturbation analysis*

The structure of the weakly nonlinear analysis above threshold is as follows: the dynamo bifurcates from a flow field $\vec{v}_c$ at $R_m = R_{mc}$. We write (135) in the form

$$L \cdot \vec{B}_0 = 0, \tag{137}$$

where $\vec{B}_0$ is the neutral mode at threshold and L is a linear operator that depends on the bifurcation structure (stationary or Hopf bifurcation). Slightly

above threshold, we have

$$\vec{v} = \vec{v}_f + \epsilon \vec{v}_1 + \cdots ,\tag{138}$$

where $\vec{v}_f = \vec{v}_c + \epsilon \vec{v}_p + \cdots$, with $\epsilon = (R_m - R_{mc})/R_{mc} \ll 1$. $\epsilon \vec{v}_p$ is the order ϵ velocity correction due to the driving of the fluid slightly above threshold. $\epsilon \vec{v}_1$ is the leading order flow distortion by the Laplace force. We have for $\vec{B}$

$$\vec{B} = \sqrt{\epsilon} \left(\vec{B}_0 + \epsilon \vec{B}_1 + \cdots \right).\tag{139}$$

We first compute $\vec{v}_1$ from (136) at order ϵ,

$$\frac{\partial \vec{v}_1}{\partial t} + (\vec{v}_c.\nabla)\vec{v}_1 + (\vec{v}_1.\nabla)\vec{v}_c = -\frac{1}{\rho}\nabla\left(p_1 + \frac{B_0^2}{2\mu_0} \right) + \nu\Delta\vec{v}_1 + \frac{1}{\mu_0\rho}(\vec{B}_0 \cdot \nabla)\vec{B}_0.\tag{140}$$

If $P_m \gg 1$, the flow is laminar at the dynamo threshold, and the Laplace force is mostly balanced by the modification of the viscous force, thus

$$v_1 \propto \frac{B_0^2 L}{\mu_0 \rho \nu}.\tag{141}$$

We get from (135) at order ϵ,

$$L \cdot \vec{B}_1 = \frac{\partial \vec{B}_0}{\partial T} - \nabla \times (\vec{v}_p \times \vec{B}_0) - \nabla \times (\vec{v}_1 \times \vec{B}_0),\tag{142}$$

where $T = \epsilon t$ is the slow time scale of $\vec{B}_0$ slightly above threshold. The amplitude equation for $\vec{B}_0$ that governs the saturation of the magnetic field is obtained by applying the solvability condition to (142),

$$\left\langle \vec{C}|\frac{\partial \vec{B}_0}{\partial T} \right\rangle = \left\langle \vec{C}|\nabla \times (\vec{v}_p \times \vec{B}_0) \right\rangle + \left\langle \vec{C}|\nabla \times (\vec{v}_1 \times \vec{B}_0) \right\rangle,\tag{143}$$

where $\vec{C}$ is the eigenvector of the adjoint problem (see the example below). The first term on the right hand side of (143) corresponds to the linear growth rate of the magnetic field whereas the second describes the nonlinear saturation due to the modified velocity field $\vec{v}_1$. For nonlinearly saturated solutions, we thus get $v_p \propto v_1$. In the vicinity of threshold, $\mu_0 \sigma L(v_f - v_c) \propto R_m - R_{mc}$, and we obtain

$$B^2 \propto \frac{\rho\nu}{\sigma L^2}\left(R_m - R_{mc} \right).\tag{144}$$

We call (144) the "laminar scaling", characterized by the fact that $B \to 0$ if $\nu \to 0$ with all the other parameters fixed. In the next section we derive this formula for a Ponomarenko type flow. The main difficulty of this type of computation is that, in general, the dynamo problem is not self-adjoint and that the adjoint problem is not a dynamo problem [56].

7.1.2. *Saturation of the Ponomarenko dynamo*

We study here the simplest possible configuration obtained by slightly modifying Ponomarenko's original configuration. We consider that the rotating cylinder is hollow and filled with a liquid metal with the same conductivity. This gives a very simple flow, solid body rotation and translation, which is the simplest way to avoid turbulence at dynamo onset. The kinematic dynamo problem is thus the same as the one studied by Ponomarenko. However, above the dynamo threshold, the flow is modified by the Laplace force and is expected to saturate the growth of the magnetic field.

In the framework of the last section we calculate the important terms involved in the amplitude equation (143). Note that $\vec{v}_c$ and $\vec{v}_p$ are both solid body rotation and translation. More precisely, we have

$$\vec{v}_f = \frac{R_m - R_{mc}}{R_{mc}} \vec{v}_c$$

that just means that the cylinder is moving faster than at criticality with all its velocity components simply proportional to R_m. We use R, $\mu_0 \sigma R^2$, $(\mu_0 \sigma R)^{-1}$, $\rho(\mu_0 \sigma R)^{-2}$ and $\sqrt{\mu_0 \rho}/\mu_0 \sigma R$ as units for length, time, velocity, pressure and magnetic field. Equation (137) gives

$$\vec{B}_0(t, T) = A(T) \times \vec{B}_p(r, \theta, z, t) + c.\ c. \tag{145}$$

$$= A(T) \times \vec{b}_p(r) \exp i(m\theta + kz + \omega_0 t) + c.\ c. \tag{146}$$

where $c.c.$ stands for complex conjugated.

We then have to calculate the adjoint operator of L. We first have to define a scalar product on the manifold of the magnetic fields. The simplest choice is space integration of the vectorial scalar product (up to a multiplicative constant).

For fields $\vec{B}_a$ and $\vec{B}_b$ of the form (85), we define

$$\langle B_a | B_b \rangle = \int_0^\infty \vec{b}_a^*(r) \cdot \vec{b}_b(r)\ r dr\,. \tag{147}$$

The adjoint operator is defined by

$$\langle B_a | L B_b \rangle = \left\langle L^\dagger B_a | B_b \right\rangle\,. \tag{148}$$

Simple integrations by parts yields

$$L^\dagger \vec{C} = -i(\omega_0 + \mu\Gamma(r))\vec{C} - \Delta\vec{C} + D_l^\dagger \vec{C} \tag{149}$$

where

$$D_l^\dagger = \begin{pmatrix} 0 & R\omega\delta(r-1) & V\delta(r-1) \\ 0 & 0 & 0 \\ 0 & 0 & 0 \end{pmatrix}\,. \tag{150}$$

This last operator, related to the boundary conditions, is the transposed of the one of the initial problem. Apart for this term, the adjoint operator can be obtained with the transformation $\mu \rightarrow -\mu$ and $\omega_0 \rightarrow -\omega_0$, i.e. by time reversal. But the boundary conditions must be taken into account and change drastically the problem. Looking for the elements of the kernel of $L^\dagger$, we see that the z-component of the field is not anymore coupled to the others and is solution of a diffusive Bessel equation without source term; the boundary conditions being zero at infinity and finite at the origin, the only solution is then zero and the elements of the kernel of the adjoint problem have no z-component (see Figure 12). Note that they are not even divergence free which means that they are not magnetic fields, a possibility already mentioned by Roberts [56].
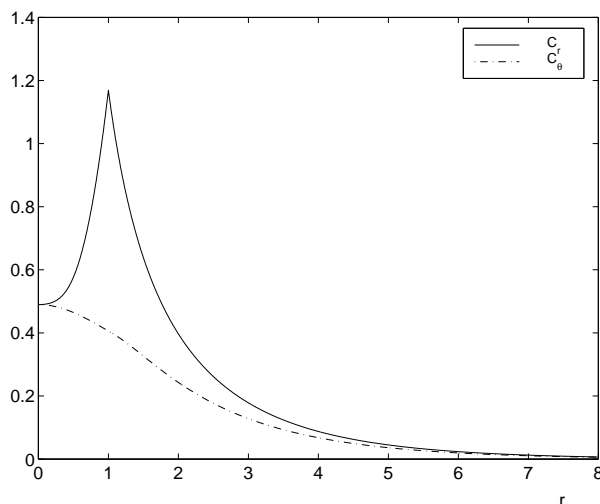

Figure 12.   Kernel of the adjoint problem for $R_m^c = 17.72$ and $R_o = 1.314$. Absolute value of the r and θ-components, the z-component is zero.

Once the adjoint problem has been solved, the amplitude equation is derived from equation (143) and takes the form

$$\frac{dA}{dt} = \alpha A + \beta |A|^2 A, \tag{151}$$

as usual for the normal form of a Hopf bifurcation. The first term of the

second member α is the linear growth rate and its expression is

$$\alpha = -\frac{R_m - R_{mc}}{R_{mc}} \ \frac{i\langle\vec{C}|\mu|\vec{B}_0\rangle + R^2\omega\,\vec{c}_\theta^*(1)\vec{b}_{pr}(1)}{\left\langle\vec{C}|\vec{B}_0\right\rangle}\,. \qquad (152)$$

With the parameter values corresponding to the minimum R_{mc}, we obtain $\alpha = (0.0268 + 0.00176\,i)(R_m - R_{mc})$. The same result can be derived by expanding Ponomarenko's equation (95).

The next coefficient requires the calculation of $\vec{v}_1$ from (140). Here $\vec{v}_1$ is the sum of three terms having a dependence $\exp 2i(m\theta + kz + \omega_0 t)$, $\exp -2i(m\theta + kz + \omega_0 t)$ or independent of θ, z and t. The main contribution to β comes from this last term and we plot the θ and z-components of $\vec{v}_1$ in Figure (13) for $P_m = 1$ and $|A|^2 = 1$. Note that this term is inversely proportional to P_m and has no radial component. With this velocity perturbation, we get $\beta = (-0.0135 - i\,0.0061)/P_m$.
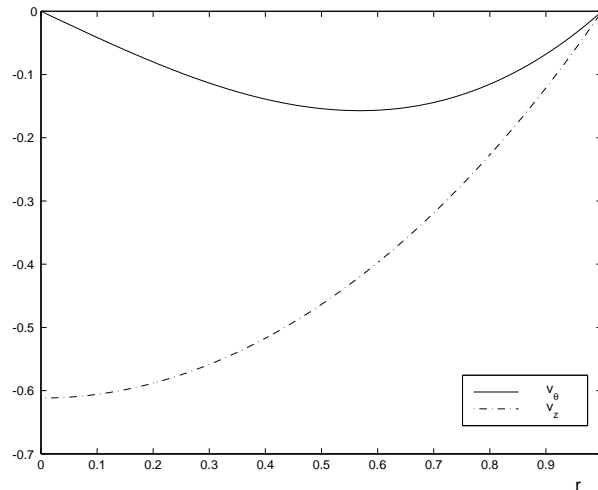

Figure 13.   Velocity perturbation solution of equation (140) for $Pm = 1$ and $|A|^2 = 1$.

The first result of this calculation is that the bifurcation is supercritical because $Re(\beta) < 0$, thus the leading order nonlinear effects tend to saturate the growing magnetic field. Physically, as we can see in Figure (13), the Laplace force slows down the motion and hence diminishes the induction.

The amplitude at saturation can be calculated. We get $|A|^2 = 1.98\,P_m\,(R_m - R_{mc})$ and turning back to dimensional variables, we obtain for the magnetic field at saturation B_{sat} and perturbation in velocity

field at saturation v_{1sat}

$$\vec{B}_{sat} = A\frac{\eta\sqrt{\rho\mu_o}}{R}\vec{B}_p + cc = 2.82\sqrt{\frac{\rho\nu}{\sigma R^2}}\sqrt{R_m - R_{mc}}\,Re(\vec{B}_p)\,, \qquad (153)$$

$$\vec{v}_{1sat} = \frac{1.98}{\mu_o\sigma R}(R_m - R_{mc})\,\vec{v}_1\,, \qquad (154)$$

where v_1 has been plotted in Figure (13). The magnetic energy has the form of equation (144), what we called the laminar scaling because the Laplace force is balanced by the perturbation in velocity through a viscous term. Close to onset, there is obviously no equipartition of energy because the magnetic energy tends to zero with $R_m - R_{mc}$ while the kinetic energy is finite. There is neither any simple balance between viscous dissipation and Joule dissipation. For Joule dissipation we have $P_j \propto \int j^2 dV \propto \int (\nabla \times B)^2 dV \propto (R_m - R_{mc})$. Concerning viscous dissipation P_ν, it is proportional to the square of the stress tensor. This tensor is linear in the total velocity and is thus proportional to $\vec{v}_1$ because the stress tensor of $\vec{v}_f$ is zero (solid body rotation and translation). Hence $P_\nu \propto \vec{v}_1^2 \propto (R_m - R_{mc})^2$. In this particular case, with no viscous dissipation at onset, we observe that most of the input power is dissipated by Joule effect close to the dynamo onset. In more complex laminar flows, Joule dissipation is of course negligible compared to viscous dissipation just above the dynamo threshold.

More realistic helical flow geometries have been considered [57] but the saturating magnetic field has been computed only in the limit $Re \gg R_m \gg 1$ for which it is difficult to have controlled approximations. However, the result also shares the main property of the laminar scaling, $B \to 0$ if $\nu \to 0$ with all the other parameters fixed.

7.1.3. *Saturation of dynamos driven by the α-effect*

Saturation of a dynamo generated by the α-effect may involve the generation of a large scale flow generated by the large scale magnetic field [58]. We have already mentioned that if a large scale flow is not forbidden by the geometrical configuration, it is likely to exist without magnetic field and to play a role already at the level of the kinematic dynamo problem. On the contrary, if any large scale flow is forbidden, as in the Karlsruhe experiment, the saturation is due to the modification of the small scale velocity field which reduces the elecromotive force related to the α-effect. In that case, the perturbation method based on scale separation can be easily extended to the study of the dynamic dynamo problem, as shown in the case of the G. O. Roberts' flow [59,60]. The mean field equation (105) is unchanged but the mean electromotive force $\langle\vec{v}\times\vec{b}\rangle$ should be calculated using

both equation (106) and the Navier-Stokes equation (136). The simplest way to generate G. O. Roberts' flow is to add a body force $\vec{f} = -\nu\Delta\vec{v}_0$ to (136) where $\vec{v}_0$ is given by (110). We have to leading order

$$\nu_m\Delta\vec{b} \approx -(\vec{B}_0\cdot\vec{\nabla})\vec{v},$$
$$\nu\Delta\vec{v} + \frac{(\vec{B}_0\cdot\vec{\nabla})\vec{b}}{\rho\mu_0} + \vec{f} \approx 0\,. \qquad (155)$$

The first equation is formally unchanged compared to the kinematic calculation although $\vec{v}$ is not given any more but should be obtained by solving the linear system (155). The velocity field $\vec{v}_0$ in the absence of magnetic field is modified by the Laplace force. Note that $(\vec{B}\cdot\vec{\nabla})\vec{B} \approx (\vec{B}_0\cdot\vec{\nabla})\vec{b}$ up to terms of order $\sqrt{l/L} \ll 1$ from the assumption of scale separation. Solving (155), we get for the electromotive force

$$\langle\vec{v}\times\vec{b}\rangle \approx \frac{UV}{\nu_m k}\begin{pmatrix} \frac{1}{\left(1+\frac{\sigma B_1^2}{\rho\nu k^2}\right)} & 0 & 0 \\ 0 & \frac{1}{\left(1+\frac{\sigma B_2^2}{\rho\nu k^2}\right)} & 0 \\ 0 & 0 & 0 \end{pmatrix}\vec{B}_0\,. \qquad (156)$$

We thus find that the α-effect saturates when the magnetic field amplitude increases because of the action of the Laplace force on the velocity field. This saturation should not be confused with the one observed for large U in (117) which is a linear effect due to flux expulsion. It is also clear that the level of saturation of the magnetic field is the one given by the laminar scaling. Therefore, we observe that this scaling is not restricted to flows generated by moving boundaries. It occurs here for flows driven by a body force. Defining

$$\tilde{B}_i^{\,2} = \frac{\sigma B_i^2}{\rho\nu k^2}, \qquad (157)$$

we obtain from the mean field equation (105)

$$\frac{\partial\tilde{B}_1}{\partial T} = -\alpha\frac{\partial}{\partial Z}\left[\frac{\tilde{B}_2}{(1+\tilde{B}_2^2)^2}\right] + \nu_m\frac{\partial^2\tilde{B}_1}{\partial Z^2}\,, \qquad (158)$$

$$\frac{\partial\tilde{B}_2}{\partial T} = -\alpha\frac{\partial}{\partial Z}\left[\frac{\tilde{B}_1}{(1+\tilde{B}_1^2)^2}\right] + \nu_m\frac{\partial^2\tilde{B}_2}{\partial Z^2}\,. \qquad (159)$$

Numerical simulation of these equations shows that the magnetic field cascades to large spatial scales during the saturation process [59].

In the case of an isotropic flow, a nonlinear evolution equation for the mean field can be easily obtained by symmetry considerations. We get

$$\frac{\partial \vec{B}_0}{\partial T} = \alpha \vec{\nabla} \times \left(1 - \gamma \vec{B}_0^2\right) \vec{B}_0 + \nu_t \Delta \vec{B}_0 \,. \tag{160}$$

Similarly, for a flow of the type $\vec{v}(x, y)$ without preferred direction in the $x - y$ plane, we define $A = B_1 + iB_2$ and get

$$\frac{\partial A}{\partial T} = -i\alpha \frac{\partial}{\partial Z} \left[\left(1 - \gamma|A|^2\right) A\right] + \nu_m \frac{\partial^2 A}{\partial Z^2} \,. \tag{161}$$

To our knowledge, this equation has not been studied. We do not know either if there exist other examples of hydrodynamic instabilities that lead to an amplitude equation of this form for a complex field A.

In the absence of large scale flow, we expect similar nonlinearities in the case of α-dynamos generated by small scale turbulent fluctuations. Phenomenological descriptions leading to equations of the form (160) have been proposed [61,62,63]. We do not expect however that γ corresponds to the laminar scaling when the Reynolds number of the flow is large (see below). Different scaling laws have been also proposed in relation with the helicity injection rate and dynamics.

7.2. Saturation in the high Re or small P_m limit

7.2.1. Dimensional arguments

We show now that we can take advantage of the characteristics of experimental dynamos to find the correct scaling of the magnetic field above the dynamo threshold [64]. We showed in the previous section that most experimental dynamos should:

- (i) bifurcate from a strongly turbulent flow regime,
- (ii) operate in the vicinity of their bifurcation threshold.

Although (i) makes almost impossible any realistic analytical calculation or direct numerical simulation, the above two characteristics allow an estimation of the nonlinearly saturated magnetic field above R_{mc} using dimensional analysis. Our goal is thus to find the expression of B as a function of ρ, ν, μ_0, σ, L and V. We have three independent parameters, R_m, P_m and for instance the square of the Lundquist number, $B^2 \mu_0 (\sigma L)^2/\rho$, thus we have in general

$$\frac{B^2 \mu_0 (\sigma L)^2}{\rho} = f(R_m, P_m), \tag{162}$$

where f is an arbitrary function at this stage. We can find its form using the above properties: (i) implies that the momentum is mostly transported

by turbulent fluctuations. Consequently, using the basic assumption of fully developed turbulence, we can neglect the kinematic viscosity, thus P_m. (ii) implies that the dependence of B^2 in R_m is proportional to $R_m - R_{mc}$, as expected for a supercritical bifurcation close to threshold. In other words, V is not a free parameter anymore, but should take approximately the value corresponding to the dynamo threshold. Thus, (i) and (ii) reduce the number of parameters from 6 to 4, and the saturated value of the magnetic field can be obtained using dimensional analysis

$$B^2 \propto \frac{\rho}{\mu_0(\sigma L)^2} \, (R_m - R_{mc}). \tag{163}$$

There is no paradox in the fact that the saturated magnetic field is inversely proportional to the square electric conductivity and to the square of the typical lengthscale of the flow. This does not mean that one should have σ and L small in order to observe large values of B since $R_m = R_{mc}$ will be then achieved for a larger flow velocity. Using the typical velocity V_c at dynamo threshold, we can write (163) in the form, $B^2/\mu_0 \rho V_c^2 \propto (R_m - R_{mc})/R_{mc}^2$, which shows that the system is very far from equipartition of energy in the vicinity of the dynamo threshold. We emphasize also, that the interaction parameter, i.e. the ratio of the Laplace force to the pressure force driving the flow, is much smaller than one.

7.2.2. *High Re dynamos close to the bifurcation threshold*

For $P_m \ll 1$ or $Re \gg 1$, we can recover the "turbulent scaling" (163) using the structure of the perturbation analysis presented for laminar dynamos. The only difference is that if $Re \gg 1$, we have to balance the Laplace force with the inertial instead of the viscous terms in (140). We thus get $B_{laminar} \propto B_{turbulent} P_m^{1/2}$, consequently the two scalings strongly differ for experiments using liquid metals ($P_m < 10^{-5}$).

It may be instructive to replace ν by the turbulent viscosity, $\nu_t \propto VL$, in the laminar scaling (144). Using $V \approx R_{mc}/\mu_0 \sigma L$, we have

$$B^2 \propto \frac{\rho \nu_t}{\sigma L^2} \, (R_m - R_{mc}) \propto \frac{\rho}{\mu_0(\sigma L)^2} \, (R_m - R_{mc}) \, . \tag{164}$$

We thus recover the turbulent scaling. However, the above dimensional analysis does not require to make any assumption about the expression of the turbulent viscosity and is thus clearer.

The Karlsruhe [42] and Riga [37] experiments have recently reported values of the saturated mean magnetic field of order 10 mT roughly 10% above threshold. Both experiments used liquid sodium ($\mu_0 \sigma \approx 10 \, m^{-2}s$, $\rho \approx 10^3 \, kg \, m^{-3}$). The inner diameter of the Riga experiment is $L = 0.25 \, m$.

The spatial periodicity of the flow used in the Karlsruhe experiment is of the same order of magnitude, within a cylinder of radius 0.85 m and height 0.7 m. The presence of two length scales in the Karlsruhe experiment makes the comparison with our analysis more difficult, but we can easily compare the results of the Riga experiment with our "turbulent" (163) and "laminar" scalings (144), that predict a saturated field of order $10\,mT$ (respectively $10\,\mu T$). Taking into account the qualitative nature of our analysis, we conclude that the "turbulent scaling" is in agreement with the experimental observations whereas the "laminar scaling" predicts a field that is orders of magnitude too small. The "turbulent scaling" also gives a correct order of magnitude for the Karlsruhe experiment if its spatial period is taken as the relevant lengthscale in (163). We thus note that the above experiments display a very interesting feature: turbulent fluctuations can be neglected when computing the dynamo threshold; indeed, as said in the previous section, the observed thresholds are in rather good agreement with the ones predicted by solving the kinematic dynamo problem for the mean flow alone. However, the high value of Re has a very strong effect on the value of the saturated magnetic field above the dynamo threshold.

7.2.3. Effect of rotation

It is also tempting to apply the above arguments to the geodynamo. Indeed, contrary to stellar or galactic dynamos that involve R_m very large compared to R_{mc}, it is likely that for the Earth, R_m is at most a few times R_{mc}. Several models have been considered in the past, all involving laminar flows with scale separation, and the saturated magnetic field has been computed using a weakly nonlinear analysis [65,66,67,68]. Although these models involve more dimensionless parameters than the system of equations (45, 21) because of the convective driving of the flow, the rotation of the Earth and the different length scales of the basic laminar flow, most of them share the property of our "laminar scaling", i.e. $B \to 0$ if $\nu \to 0$ with all the other parameters fixed. As mentioned above, this occurs in a laminar flow as soon as the Laplace force is balanced by the modification of the viscous force in (140). In the case of rapidly rotating fluids, the Coriolis term, $-2\vec{\Omega} \times \vec{v}$ should be taken into account in (140). If we get $\vec{v}_1$ by balancing the Laplace force with the modification of the Coriolis force, we obtain for the saturated magnetic field in the vicinity of threshold

$$B^2 \propto \frac{\rho\Omega}{\sigma}\,(R_m - R_{mc}).\qquad(165)$$

In the case of the Earth core, $\sqrt{\rho\Omega/\sigma} \approx 10$ gauss, thus (16) gives a reasonable order of magnitude of the Earth field if $R_m - R_{mc}$ is small enough. The other scalings (144) and (163) give too small values of the field even if L is chosen small compared to the radius of the Earth core. In the context of the geodynamo, the prefactors in (144) and (165) are called the "weak field" (respectively "strong field") scalings [69]. Note however that the full expression (165) does not correspond to the "strong field" balance of the geodynamo $\sigma B^2 \approx \rho\Omega$. Our scaling (165) may be obtained in the vicinity of the dynamo threshold if one assumes that the Stokes force is negligible in (140) whereas it is believed that the "strong field" regime of the geodynamo occurs at finite amplitude via a subcritical bifurcation from the "weak field" one [69].

8. Conclusion

Decades after the discovery of the first analytic examples of laminar fluid dynamos, self-generation of a magnetic field by a flow of liquid sodium has been reported by the Karlsruhe [42] and Riga [37] groups. Although there were no doubts concerning laminar Roberts-type or Ponomarenko-type dynamos, these experiments have raised interesting questions about the influence of turbulent fluctuations on the dynamo threshold and on the saturation level of the magnetic field. We have explained some of the observed features in sections 6 and 7 but many aspects of linear and nonlinear fluid dynamos still deserve experimental and theoretical studies.

- Effect of turbulence on dynamo threshold

We have shown that small turbulent fluctuations do not efficiently shift the dynamo threshold obtained as if the mean flow were acting alone. This is likely to be the case of many geometrically constrained flows for which the turbulence level is small, less than 10 to 20% for instance. The threshold shift being of second order in the amplitude of the fluctuations, their effect is likely to remain smaller than the one of other approximations made when numerically solving the kinematic laminar dynamo problem (taking into account the exact boundary conditions for instance).

Turbulent fluctuations may have a much stronger effect in flows without geometrical constraints. There are also configurations in which they cannot be neglected because the mean flow alone is not a dynamo. It would be of great interest to observe self-generation primarily due to turbulent fluctuations but this remains a great experimental challenge. From the theoretical viewpoint, the problem is to understand how a magnetic field with a non-zero coherent part $\langle \vec{B}(\vec{r}) \rangle$ can be amplified by a random velocity field. Are

there small scale (i.e. with $\langle \vec{B}(\vec{r}) \rangle = 0$), respectively large scale dynamos, depending on the statistical properties of the turbulent fluctuations? From the mathematical viewpoint, it would be interesting to have rigorous results on bifurcations of systems described by partial differential equations with random coefficients in order to test the validity of mean field dynamo models.

- Saturation of the magnetic field above dynamo threshold.

We emphasize that the correct evaluation of the dominant transport mechanism for momentum is essential to estimate the order of magnitude of the saturated magnetic field above dynamo threshold. The reason is that it determines the flow distortion by the Laplace force and thus the saturation mechanism of the field. A laminar model of the flow thus generally leads to a wrong estimate of the magnetic field amplitude although it sometimes correctly predicts the dynamo threshold. It would be interesting to test the validity of the scaling law (163) we have proposed for the existing laboratory experiments. This has not been done yet, but may be achieved both in Karlsruhe and Riga experiments by varying the temperature of liquid sodium and thus its conductivity σ. Another fundamental experiment in the context of the geodynamo would be to observe the transition from (163) to (165) for a rapidly rotating flow.

- Dynamics of the magnetic field above dynamo threshold.

Magnetic fields of astrophysical objects may be found to be almost time-periodic, like in the sun, or nearly stationary i.e. very slowly varying, like for the Earth magnetic field between two successive reversals. Although the solar dynamo may be far above threshold, it is tempting to connect this temporal behavior with the nature of the dynamo bifurcation which can be either a stationary bifurcation or a Hopf bifurcation in the simplest generic cases. It should be noted that both a stationary bifurcation (Karlsruhe experiment), and a Hopf bifurcation (Riga experiment) have been observed so far. With these simple geometry flows, we have shown that it is possible to guess the nature of the bifurcation using symmetry considerations. This is less obvious in the case of fully developed turbulent flows and it would be interesting to try to understand how is determined the dynamical regime above the dynamo onset. In particular, a central problem in the context of the geodynamo is to understand the mechanism of the field reversals. Is it realistic to describe them with low dimensional dynamical systems or are turbulent and unconstrained flows essential to generate them ?

- Statistical properties of the magnetic field fluctuations.

Large scale dynamics have not been observed so far in the Karlsruhe

and Riga experiments but both display small scale fluctuations of the magnetic field. An interesting feature is that some statistical properties of the fluctuations measured in the Karlsruhe experiment are similar to the ones observed in turbulent von Kármán flows in gallium [70] and sodium [71] below the dynamo threshold but with an externally applied magnetic field. It would be of interest to understand why. Are the field fluctuations measured in the Karlsruhe experiment just due to advection of the self-generated large scale magnetic field by the small scale turbulent fluctuations of the flow? This would lead to a much simpler description of these magnetic field fluctuations than if they were more deeply connected to the generation process itself. Advection of a passive vector field by turbulence is also a very interesting problem by itself, at an intermediate level of complexity between passive scalar advection and turbulence.

Acknowledgments

References

1. F. H. Busse, "Mathematical problems of dynamo theory", in *Applications of bifurcation theory*, 175-202, Academic Press (1977).
2. M. Ghil and S. Childress, *Topics in geophysical fluid dynamics:atmospheric dynamics, dynamo theory, and climate dynamics*, Appl. Math. Sci. vol. 60, Springer Verlag (New York, 1987).
3. P. H. Roberts, "Dynamo theory" in *Irreversible phenomena an dynamical systems analysis in geosciences*, 73, C. Nicolis and G. Nicolis eds., Reidel Publishing Company (1987).
4. P. H. Roberts and A. M. Soward, "Dynamo theory", Annu. Rev. Fluid Mech. **24**, 459 (1992).
5. P. H. Roberts, "Fundamentals of dynamo theory" in *Lectures on solar and planetary dynamos* , chap. 1, 1-57, M. R. E. Proctor and A. D. Gilbert eds., Cambridge University Press (Cambridge, 1994).
6. P. H. Roberts and G. A. Glatzmaier, 2000, "Geodynamo theory and simulations", Rev. Mod. Phys. **72**, 1081.
7. H. K. Moffatt, *Magnetic field generation in electrically conducting fluids*, Cambridge University Press (Cambridge, 1978).
8. F. Krause and K.-H. Rädler, *Mean field magnetohydrodynamics and dynamo theory*, Pergamon Press (New-York, 1980).
9. S. Childress and A. D. Gilbert, *Stretch, twist, fold: the fast dynamo*, Springer (Berlin, 1995).

10. Ya. B. Zeldovich, A. A. Ruzmaikin and D. D. Sokoloff, *Magnetic fields in astrophysics*, Gordon and Breach (New York, 1983).

11. see for instance reference [1] in P. H. Roberts and T. H. Jensen, *Phys. Fluids* **B5**, 2657 (1993).

12. J. Larmor, 1919 "How could a rotating body such as the sun become a magnet?", Rep. 87$^{\text{th}}$ Meeting Brit. Assoc. Adv. Sci., Bornemouth, Sept. 9-13, 1919, pp. 159-160, John Murray (London).

13. E. C. Bullard and D. Gubbins, GAFD **8**, 43 (1977).

14. A. Tilgner, Phys. Rev. **60**, 2949 (1999).

15. F. Pétrélis, *Thèse de doctorat*, Université Paris 6 (2002).

16. S. Chandrasekhar, *Hydrodynamic and hydromagnetic stability*, Clarendon Press (Oxford, 1961).

17. S. Fauve, C. Laroche and A. Libchaber, J. Physique Lettres **42**, 455 (1981), J. Physique Lettres **45**, 101 (1984).

18. R. Moreau, *Magnetohydrodynamics*, Kluwer Academic Publishers (Dordrecht, 1990).

19. E. P. Velikhov, Soviet Phys. JETP **36**, 995 (1959).

20. S. A. Balbus and J. F. Hawley, Astrophys. J. **376**, 214 (1991).

21. G. B. Arfken, *Mathematical methods for physicists*, Academic Press (San Diego, 1995).

22. P. Odier, J.-F. Pinton and S. Fauve, Eur. Phys. J. B **16**, 373 (2000).

23. A. Herzenberg, Philos. Trans. Roy. Soc. London A**250**, 543 (1958).

24. F. J. Lowes and I. Wilkinson, Nature **198**, 1158 (1963); **219**, 717 (1968).

25. G. E. Backus, Ann. Phys. **4**, 372 (1958).

26. T. G. Cowling, Mon. Not. Roy. Astro. Soc. **94**, 39 (1934).

27. Ya. B. Zeldovich, JETP **4**, 460 (1957).

28. W. M. Elsasser, "Induction effects in terrestrial magnetism, I. Theory", Phys. Rev. **69**, 106 (1946).

29. see for instance D. J. Ivers and R. W. James, GAFD **44**, 271 (1988) and references therein.

30. M. Nunez, SIAM review **38**, 553 (1996).

31. D. Lortz, Plasma Phys. **10**, 967 (1968).

32. Yu. B. Ponomarenko, J. Appl. Mech. Tech. Phys. **14**, 775 (1973).

33. G. O. Roberts, Phil. Trans. Roy. Soc. London A **266**, 535 (1970).

34. G. O. Roberts, Phil. Trans. Roy. Soc. London A **271**, 411 (1972).

35. A. Ruzmaikin, D. Sokoloff and A. Shukurov, J. Fluid Mech. **197**, 39 (1988).

36. A. D. Gilbert, GAFD **44**, 241 (1988).

37. A. Gailitis, O. Lielausis, E. Platacis, S. Dement'ev, A. Cifersons, G. Gerbeth, T. Gundrum, F. Stefani, M. Christen and G. Will, Phys. Rev. Lett. **86**, 3024 (2001).

38. S. Fauve, *Hydrodynamics and nonlinear instabilities*, C. Godrèche and P. Manneville editors : *Pattern forming instabilities*, pp. 387-491, Cambridge University Press (Cambridge, 1998).

39. E. N. Parker, Astrophysical J. **122**, 293 (1955).

40. K.-H. Rädler, E. Apstein M. Rheinhardt and M. Schüler, Studia Geophys. Geod. **42**, 224 (1998).

41. M. Steenbeck, I. M. Kirko, A. Gailitis, A. P. Klyavinya, F. Krause, I. Ya.

Laumanis and O. Lielausis, Sov. Phys. Dok. **13**, 443 (1968).

42. R. Stieglitz and U. Müller, 2001, Phys. Fluids **13**, 561.
43. A. Lanotte, A. Noullez, M. Vergassola and A. Wirth, GAFD **91**, 131 (1999).
44. V. A. Zheligovsky, O. M. Podvigina and U. Frisch, GAFD **95**, 227 (2001).
45. A. D. Gilbert, U. Frisch and A. Pouquet, GAFD **42**, 151 (1988).
46. P. Chossat *An introduction to equivariant bifurcations and spontaneous symmetry breaking, Peyresq Lectures on Nonlinear Phenomena* (this volume).
47. C. Nore, M. E. Brachet, H. Politano and A. Pouquet, Phys. Plasmas **4**, 1 (1997).
48. L. Marié, J. Burguete, F. Daviaud and J. Léorat, *Homogeneous dynamo: numerical study of experimental von Karman type flows*, submitted to Eur. Phys. J. B (2002).
49. J. Léorat, A. Pouquet and U. Frisch, J. Fluid Mech. **104**, 419 (1981).
50. T. John, R. Stannarius and U. Behn, Phys. Rev. Lett. **83**, 749 (1999).
51. R. Berthet, A. Petrossian, S. Residori, B. Roman and S. Fauve, "Effect of multiplicative noise on parametric instabilities", to be published in Physica D (2002).
52. see for instance, N. Platt, E.A. Spiegel and C. Tresser, Phys. Rev. Lett. **70**, 279 (1993) and references therein.
53. D. Sweet, E. Ott, J. Finn, T. M. Antonsen and D. Lathrop, Phys. Rev. E **63**, 066211 (2001).
54. A. B. Reighard and M. R. Brown, Phys. Rev. Lett. **86**, 2794 (2001).
55. A. Nunez, F. Pétrélis and S. Fauve, "Saturation of a Ponomarenko type fluid dynamo", in *Dynamo and dynamics, a mathematical challenge*, P. Chossat et al. (eds.), 67-74, Kluwer Academic Publishers (2001).
56. P. H. Roberts, J. Math. Anal. Appl. **1**, 195 (1960).
57. A. P. Bassom and A. D. Gilbert, J. Fluid Mech. **343**, 375 (1997).
58. W. V. R. Malkus and M. R. E. Proctor, J. Fluid Mech. **67**, 417 (1975).
59. A. D. Gilbert and P. L. Sulem, GAFD **51**, 243 (1990).
60. A. Tilgner and F. H. Busse, "Saturation mechanism of a model of the Karlsruhe dynamo", in *Dynamo and dynamics, a mathematical challenge*, P. Chossat et al. (eds.), 109-116, Kluwer Academic Publishers (2001).
61. R. H. Kraichnan, Phys. Rev. Lett. **42**, 1677 (1979).
62. M. Meneguzzi, U. Frisch and A. Pouquet, Phys. Rev. Lett. **47**, 1060 (1981).
63. A. V. Gruzinov and P. H. Diamond, Phys. Rev. Lett. **72**, 1651 (1994).
64. F. Pétrélis and S. Fauve, Eur. Phys. J. B **22**, 273 (2001).
65. S. Childress and A. M. Soward, Phys. Rev. Lett. **29**, 837 (1972).
66. A. M. Soward, Phil. Trans. R. Soc. Lond. **A 275**, 611 (1974).
67. F. H. Busse, Generation of planetary magnetism by convection, Phys. Earth Planet. Inter. **12**, 350-358 (1976).
68. Y. Fauterelle and S. Childress, GAFD **22**, 235 (1982).
69. P. H. Roberts, GAFD **44**, 3 (1988).
70. P. Odier, J.-F. Pinton and S. Fauve, Phys. Rev. E **58**, 7397 (1998).
71. M. Bourgoin, L. Marié, F. Pétrélis, C. Gasquet, A. Guigon, J. B . Luciani, M. Moulin, F. Namer, J. Burgete, A. Chiffaudel, F. Daviaud, S. Fauve, P. Odier, J. F. Pinton, Phys. Fluids 14, 3046 (2002).